Investigation and model development for operational modes of a Unified Power Flow Controller

by

Forough Mahmoodianfard

A Thesis
submitted to the Faculty of Graduate Studies,
in Partial Fulfilment of the Requirements for the degree of

Master of Science
in
Electrical and Computer Engineering

Department of Electrical and Computer Engineering
University of Manitoba
Winnipeg, Manitoba R3T 5V6 Canada

Investigation and model development for operational modes of a Unified Power Flow Controller

by

Forough Mahmoodianfard

A Thesis
submitted to the Faculty of Graduate Studies,
in Partial Fulfilment of the Requirements for the degree of

Master of Science
in
Electrical and Computer Engineering

Abstract

The focus of this research is on deriving small signal stability models for different Flexible AC Transmission Systems (FACTS) devices by introducing a simple systematic method that is applicable to any dynamic device.

Two different small signal models for Unified Power Flow Controllers are introduced. One model is called the power control mode and the other model is the voltage control mode. The two models are compared from transient stability point of view to show the necessity of developing both models for UPFC.

The thesis also shows how to derive the small signal stability model of Static Synchronous Compensator, as the shunt branch of UPFC. The small signal stability models of both devices are then validated to ensure the accuracy of the derived models. STATCOM and UPFC power control mode are validated against PSCAD. The UPFC voltage control mode is validated against nonlinear solution of system equations.

Acknowledgements

Many thanks to the following persons for their role in the completion of this thesis.

- My dear advisor, professor Annakkage who helped me a lot during my research.
- My examination committee who made time to read my thesis.
- My parents and family who helped me to grow and supported me through every single steps in my life.
- And last but not least, my dear friends who are like a family to me and were with me in all hard situations I had to deal with.

This research has been supported by grants of Manitoba Hydro and NSERC.

Contents

List of Tables

List of Figures

1 Introduction

1.1 Flexible AC Transmission (FACTS) Controllers

Almost all power supply systems in the world are connected together. This interconnected configuration helps to supply cheaper electricity and make the whole system more reliable. A transmission system is necessary because it not only delivers the generated power to loads but also minimizes total power generation capacity and fuel cost [3].

The flow of power in an AC system depends on the line impedances. Consider a simple AC system with a set ofparallel line connecting the generation to the load. Power flow in such a system is based on the inverse of line impedances, i.e., the line with the smaller impedance carries more power. This may overload the line with lower impedance. Therefore, some sort of power flow controller in the line is needed. FACTS controllers can fill this need for the system [4]. FACTS controllers are generally divided into four categories:

- series controllers
- shunt controllers
- combined series-series controllers; and
- combined series-shunt controllers

Series controllers are any different type of impedance, such as reactor or capacitor that inject a voltage in series with the line. If the injected voltage is in phase with the line voltage, then only reactive power is injected to or absorbed from the line otherwise both active and reactive power flow would be exchanged between the line and the series controller [5], [6].

Shunt controllers, like series controllers, could be of any variable impedance, such as reactor or capacitor except that shunt devices inject current at the point of connection to the network. As it was mentioned for the series controllers, if the injected current is perpendicular to the line voltage, then only reactive power is injected to or absorbed from the network otherwise both active and reactive power flow are exchanged between the line and the shunt controller. A static synchronous compensator (STATCOM) is an example of

Table 1.1: FACTS Controllers Categories [1]

Type	Thyristor-based				converter-based			
	SVC		TCSC	PS	STATCOM	SSSC	UPFC	IPFC
	TSC	TCR						
Compensation	shunt	shunt	series	shunt	shunt	series	both	both

a shunt controller which exchanges reactive power flow with the network at the point of common coupling with the system [7], [8].

Combined series-series controllers consist of two series controllers. These controllers can be either controlled in a coordinated manner or they can be unified controllers. Unified controllers can be said to exist when all the series controllers in a given system are connected at a common DC bus. An example of a unified combined series-series controller is the Interline Power Flow Controller (IPFC) [9], [10].

Combined series-shunt controllers are a combination of series and shunt controllers. As with combined series-series controllers, combined series-shunt controllers could be either controlled in a coordinated manner or they can be unified controllers. An example of a unified series-shunt controller is the Unified Power Flow Controller (UPFC), which along with STATCOM is the focus of this thesis [11], [12].

From another point of view, the controllers can be divided into two categories based on the type of power electronics technology used in FACTS controllers; thyristor controlled and voltage source converter type (see table (1.1)) [1]. The two different categories are shown in figures (1.1) and (1.2).

Thyristor-controlled FACTS controllers are widely used in power systems. The main drawback of these devices is their limited controllability because thyristors can't be forced to turn off. A thyristor will turn off only when the current in the system changes its direction. As it can be seen from the figure (1.1), examples of thyristor-controlled devices are: Static Var Compensator (SVC), Thyristor-Controlled Series Capacitor (TCSC) and the thyristor controlled Phase-Shifter (TCPS). Each of these devices can make a change in power flow by changing a parameter in the system. The SVC changes the voltage of the bus to which

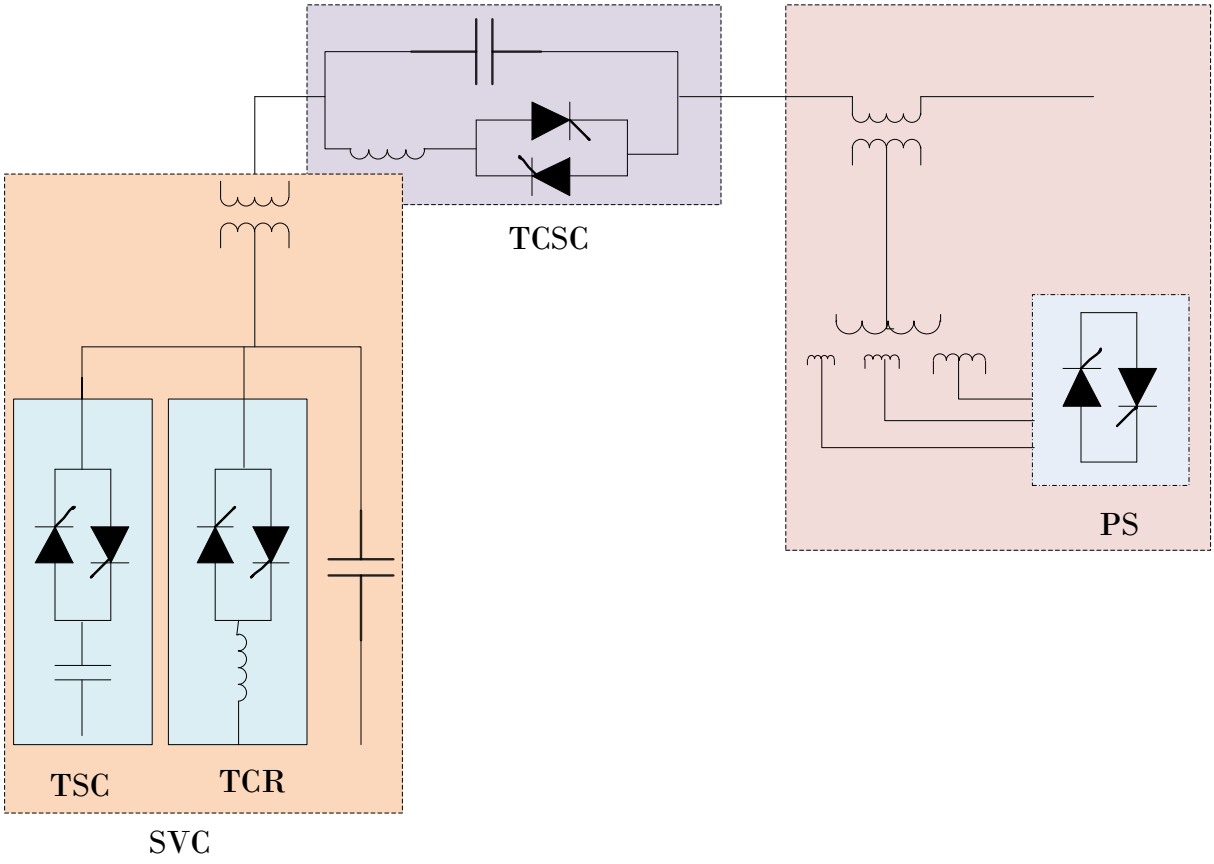

Figure 1.1: Thyristor controlled FACTS Controllers [1]

it is connected, by switching the shunt capacitors (Thyristor-Switched Capacitor: TSC) or reactors (Thyristor-Controlled Reactor: TCR). A TCSC changes the impedance in series with the line. Finally, A TCPS changes the phase angle of the line voltage by injecting some voltage in series with the line. A TCPS is like a tap-changer, but it is considerably faster compared to the tap-changer.

Figure (1.2) depicts voltage source controlled FACTS devices. Examples shown are: Static Synchronous Compensator (STATCOM), the Static Synchronous Series Compensator (SSSC), the Unified Power Flow Controller (UPFC) and the Interline Power Flow Controller (IPFC). Unlike the thyristor-controlled devices, VSC based controllers use Gate Turn-Off thyristors (GTO) or Insulated-Gate Bipolar Transistors (IGBT) in their structure. Therefore, it is possible to turn them off whenever necessary and it is one of their advantages over thyristor-

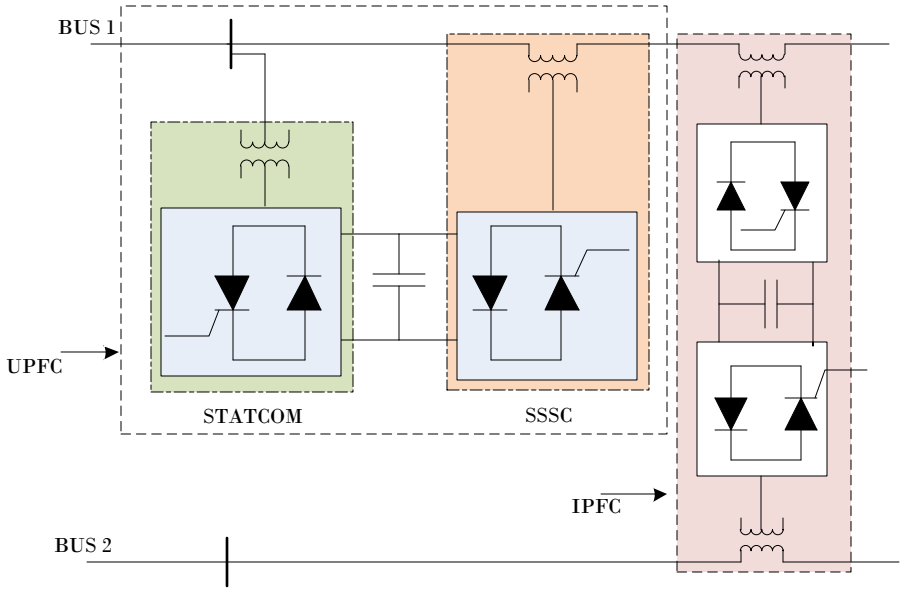

Figure 1.2: Voltage Source Controlled FACTS Controllers [1]

based controllers. These devices provide either series or shunt compensation. STATCOM, as with SVC, changes the voltage of the bus connected to it by adjusting the reactive current injection to the bus known as shunt compensation [13]. SSSC, as with TCSC, provides series compensation. It injects voltage in series with the line to change the effective impedance of the line [14], [15]. UPFC provides both series and shunt compensation by combining STATCOM and SSSC through a DC capacitor [16], [17]. It can control active and reactive power flow in the line as well as the voltage magnitude at the point of connection to the line [18]. IPFC combines two SSSCs through a DC capacitor. It provides series compensation along with real power balancing between two different lines [19].

In this thesis, STATCOM and UPFC are studied and their small signal stability models are derived.

1.2 Small Signal Stability

One of the most important aspects of a power system is it's capability to remain stable under different operating conditions. A power system is called stable if it can reach steady state after being subjected to a disturbance and none of the operating constraints reach their

limits at the new steady state. A power system can be classified into four categories based on the size of the disturbance applied to the system, the physical nature of the resulting instability mode in the system and the amount of time, device and process needed to analyze the stability [20]. A classical definition of power system stability is given in [20].

It is important to be able to distinguish between the categories in order to take the required actions to maintain the stability of the network. As it can be seen from the figure (1.3) three main categories are, voltage stability; frequency stability and rotor angle stability. Voltage stability is the ability of the system to maintain the voltage of all the buses in the system at an acceptable level at all times even after being subjected to a disturbance or contingency [21]. Frequency stability is the ability of the system to keep the frequency at a nominal value. Finally, rotor angle stability is the ability of the system to maintain the synchronism in the system after the system is subjected to a disturbance or contingency. As figure (1.3) shows, voltage and frequency stability can be both long and short term phenomenon, while rotor angle stability is a short term phenomenon. As already mentioned and from figure (1.3), it can be observed that the type of instability depends on the size of the disturbance applied to the system.

In the case of small signal stability, which is the focus of this thesis, a small disturbance is applied to the system. It's is assumed that the disturbance is small enough that the system can be linearized around the operating point. As a result of the small disturbance, the system can become unstable in two ways: (i) the generator rotor angle may increase steadily because of lack of synchronism torque, or (ii) the rotor angle may oscillate with increasing magnitude because of lack of damping torque [2]. In order to perform a small signal stability analysis, a dynamic system such as a power system should be first represented using algebraic and differential equations. In the next step, the equations must be linearzied around the steady state operating point. Then the linearized equations are transformed into frequency domain. Then, the stability of the system could be determined using frequency domain methods. To model the system for small signal stability analysis, each element of the system can be modeled using simplified assumptions. While these simpli-

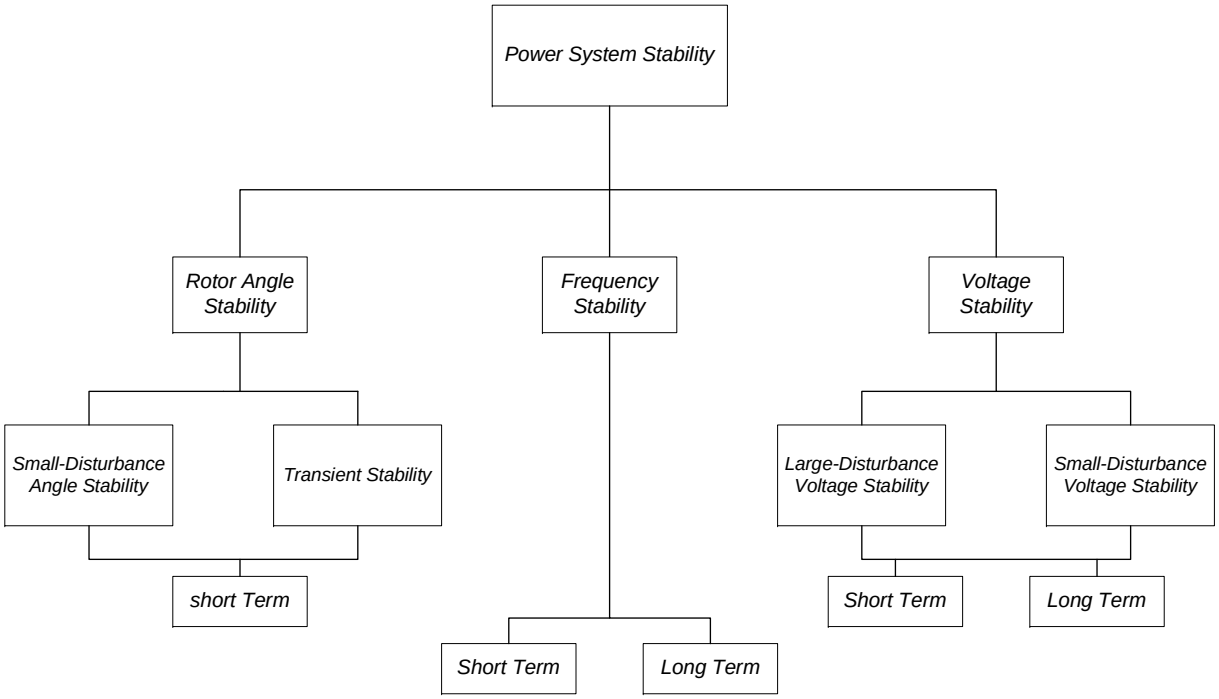

Figure 1.3: Classification of power system Stability

fied assumptions make it easy to derive a small signal model for the system, they may result in inaccurate results. Therefore, it's necessary to validate the model against a real network or a more accurate program.

In this thesis, the STATCOM and UPFC small signal models are validated against a detailed electromagnetic transient simulation program (PSCAD) and nonlinear equations. This thesis is organized as follows: Chapter (2) contains the two proposed model for the UPFC and their comparison from transient stability point of view, chapter (3) presents the step by step procedure of deriving the small signal stability model for STATCOM. Chapter (3) also contains the validation of small signal stability model against STATCOM model developed in PSCAD. Chapter (4) demonstrates the detailed computation of the UPFC small signal model for both proposed models, i.e. power control mode and voltage control mode. Then for the power control mode, the resulting small signal model is validated against PSCAD to ensure the accuracy of the model. The voltage control mode is validated against the nonlinear solution of the sample power network. Validation of the model against

EMT simulation is not presented because there were errors which could not be resolved. This thesis used a simple systematic method to model STATCOM and UPFC. However, the same steps can be taken to model other devices, such as IPFC, SSSC, etc. The same approach has also been used in the recent works of the power system group at the University of Manitoba. The HVDC converter model was developed using the same method by Chandana Karawita [22]. The wind power plant model has also been introduced taking the same approch by Hiranya Suriyaarachchi [23]. Chapter (5) concludes the thesis.

2 Introducing two different small signal models for UPFC

In this thesis, two different small signal models for UPFC are proposed. One is called P, Q control model and the other one is called the voltage control model.

The P, Q model takes a reference value for active and reactive power flow in the line and aims to maintain P and Q flowing in the line at the reference value. The two PI controllers used in this model measure the active and reactive power flow in the line individually and compare them to the reference values. Then based on the deviations from the references, they inject voltages in-phase and quadrature to the UPFC sending end bus voltage to keep the power flow in the line at the same level as the reference values.

In the voltage control model, a constant voltage is injected directly in series with the line. The injected voltage has two components. One component is in-phase with the voltage at the sending bus of the UPFC and the other component is quadrature to the same voltage. Unlike the P, Q control model, this model gets no feedback from the power flow in the line. However, the power flow in the line can be changed by changing the amount of voltage injection to the line.

The P, Q control mode has been modeled with different types of controllers such as d-q controller [1]. The voltage control mode has also been proposed previously by [24]. However, the model has not been fully validated. This chapter will demonstrate the advantages and disadvantages of both models from transient stability point of view. It will also explain the need to develope the small signal stability model for the voltage control mode of the UPFC.

2.1 Transient Stability Concept

As discussed in chapter (1), transient stability is the ability of the synchronous machines in a system to stay in synchronism after facing a disturbance. The disturbance could be a fault in the transmission system, loss of generation or a large amount of load. If the machines lose their synchronism because of a severe disturbance, it will be recognized in a few cycles

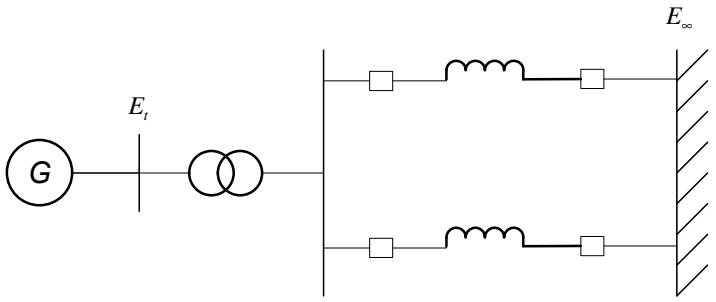

a) Single line diagram

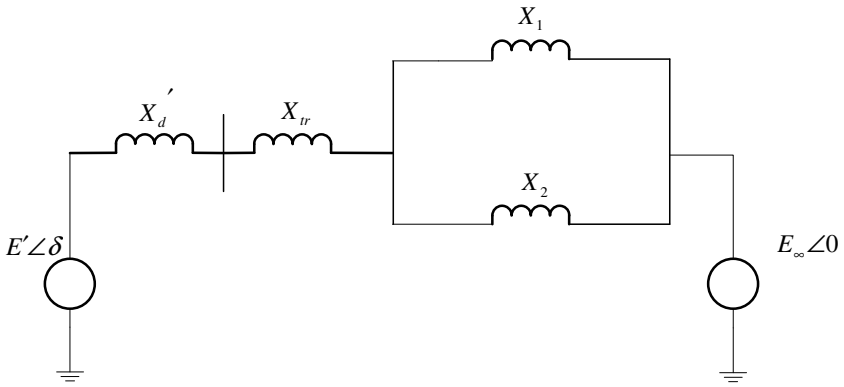

b) Equivalent circuit

Figure 2.1: Simple system for transient stability explanation

after the disturbance.

The single line diagram for the system and its equivalent circuit are as shown in figure (2.1). In order to explain transient stability concepts, a small system is considered. In this system a generator is delivering power to a large system through a set of parallel transmission lines. Note that the infinite bus voltage has been considered as the reference and the machine internal voltage is leading the infinite bus voltage by the angle δ.

To examine the behavior of the system from transient stability point of view, the swing equation given in equation (2.1) needs to be solved. However, for the simple system shown in figure (2.1), with the generator modeled as the classical model, it is possible to use the

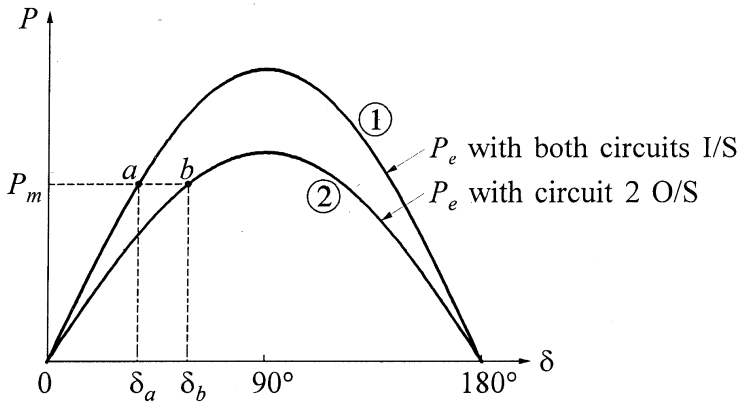

Figure 2.2: two different $P - \delta$ curve with a constant P_m [2]

power-angle relationship ($P - \delta$) curve, to investigate the operation of the system during the transient period (figure (2.2)).

$$\frac{2H}{\omega_0}\frac{d^2\delta}{dt^2} = P_m - P_e \tag{2.1}$$

For the system given in figure (2.1), P_e can be calculated from equation (2.2). In this equation, X_T is the equivalent impedance of the network between E' and E. The system reaches its steady state operating point at the angle where, P_m is equal to P_e. The $P - \delta$ curve shows how the power flow in the line changes as a result of the generator angle variation. It is assumed that the voltage at both ends of the line are constant. It can be understood from figure (2.2) that for a constant P_m the machine angle could be different for different operating conditions of the system.

$$P_e = \frac{E'E}{X_T} sin(\delta) = P_{max} sin(\delta) \tag{2.2}$$

Let us assume a fault happens at the system. If the fault happens at the sending end bus of the transmission line on the generator side, there is no power transfer from the generator to the infinite bus during the fault. The entire generator current would feed the fault. If the fault happens somewhere in one of the transmission lines, there is still some power transfer from the generator to the infinite bus.

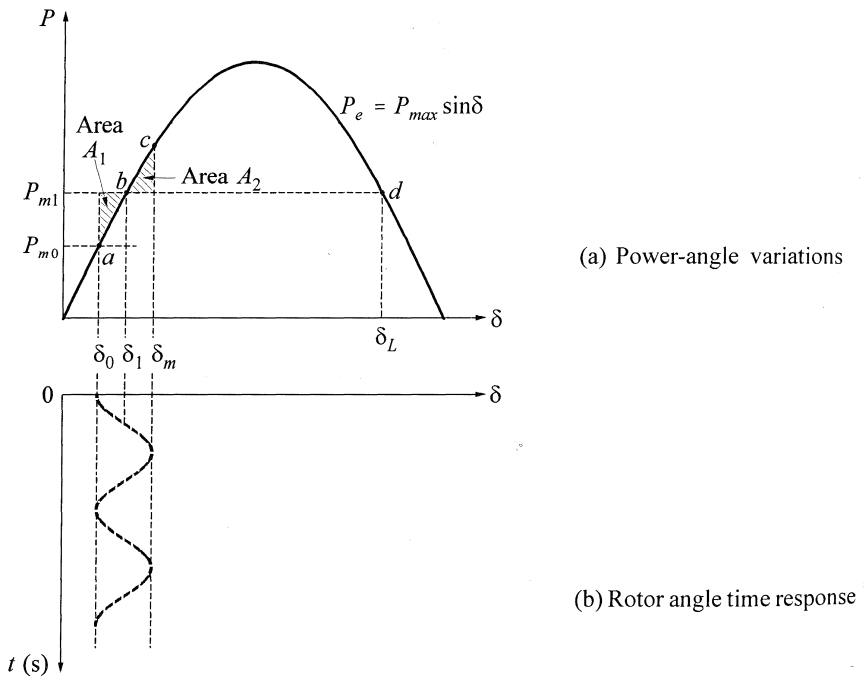

Figure 2.3: Equal-area criterion [2]

The behavior of the system before, during and after a fault can be examined by solving the swing equation. However, if the system can be simplified as the system shown in figure (2.1), the accurate behavior of the system can be predicted by just using the $P - \delta$ curve. The method which is used to foresee the transient performance of the power system by using the $P - \delta$ curve, is called the equal-area criterion.

The equal-area criterion is explained assuming a step change happens in the P_m value according to figure (2.3). According to the swing equation, if the mechanical power input (P_m) to the machine is higher than the electrical power output (P_e), the machine accelerates; or in other words gains kinetic energy. This is corresponding to area A_1 in figure (2.3). However, if P_m is smaller than P_e, the machine decelerates or loses its kinetic energy. It is equivalent to the area A_2 in the same figure. According to the equal-area criterion, the system will be transiently stable if A_2 is equal to A_1.

From figure (2.3), for $P_m = P_{m_0}$ the machine rotor angle is δ_0 and the machine is in synchronism with other machines in the system. Now assume P_m increases from P_{m_0} to

P_{m_1}. Since P_{m_1} is larger than P_e, the machine starts accelerating and as a result δ starts increasing. The operating point of the system moves from δ_0 to δ_1 along the $P-\delta$ curve. When $P_e = P_{m_1}$ there's no accelerating force. However, because the machine speed is larger than the synchronous speed of the system, δ continues increasing and machine starts decelerating. For values of δ larger than δ_1, P_e is higher than P_{m_1} and the machine loses the kinetic energy it gained before, until δ reaches its maximum value δ_m. At that moment, rotor speed is the same as synchronous speed. On the other hand, since P_e is still more than P_m the machine keeps decelerating and rotor angle reduces from its maximum value. Therefore, the operating point moves along the $P-\delta$ and goes from c to b to a. If there is no damping in the system, the rotor angle keeps oscillating between a and c.

2.2 Applying the equal-area criterion to the system including UPFC

2.2.1 System with P, Q control mode for UPFC

Figure (2.4) shows the P, Q control model which is built in PSCAD. The model will be used later as a reference to evaluate the accuracy of the developed small signal stability model.

Each model shows a different response depending on where in the system, the fault happens. We will discuss the behaviour of the P, Q control mode using the Power-angle relation presented in equation (2.2). The response of the voltage control mode is explained in details using the $P-\delta$ curve in the remaining part of this chapter. The comparison of the two models is presented at the end of the chapter.

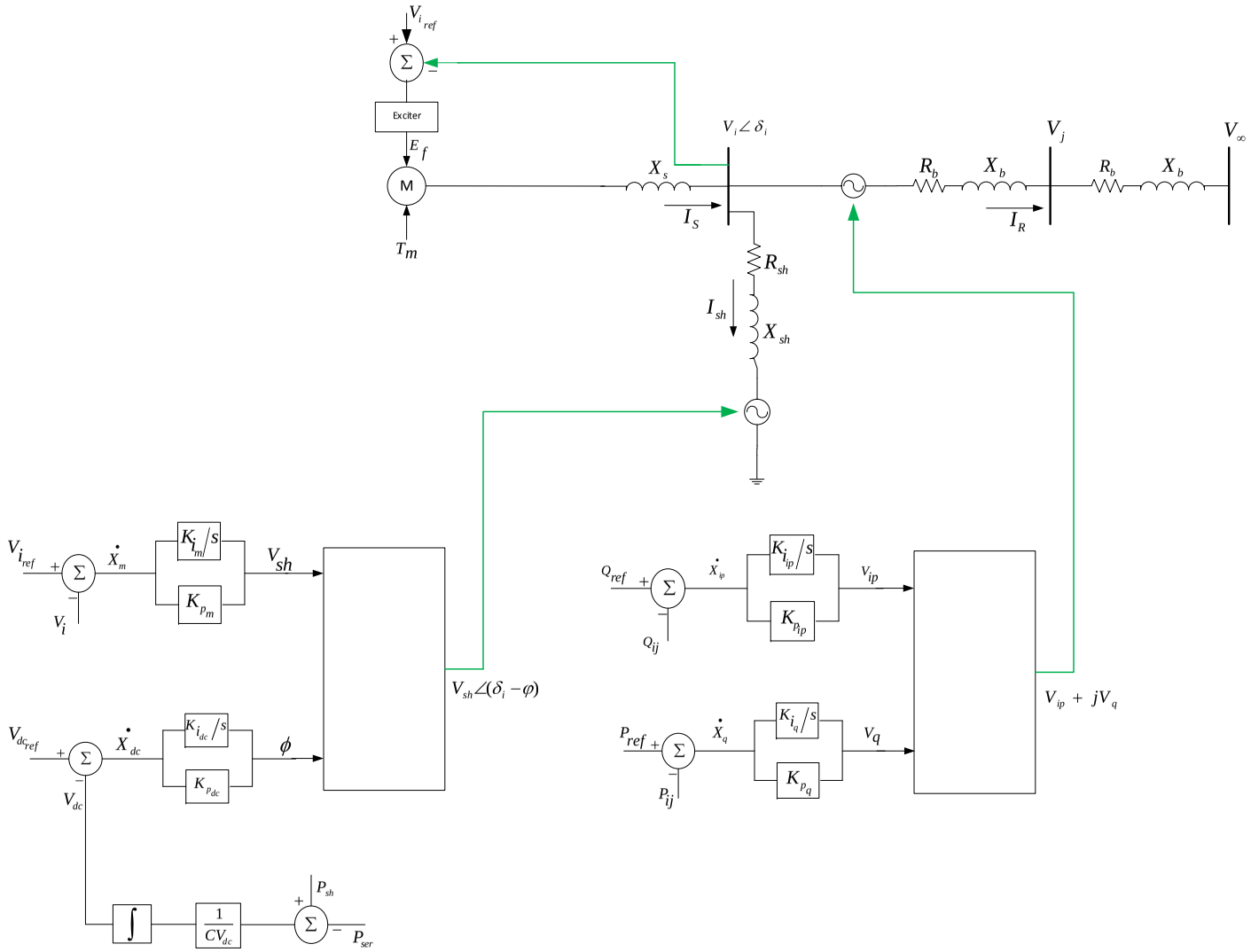

Figure 2.4: UPFC P, Q model including control parameters

In the P, Q control mode, the active and reactive power flow in the line are kept constant by the series controllers. The active power flow is measured between the sending bus of the UPFC and the infinite bus. At steady state and before any type of disturbance is imposed on the system, the sending bus voltage has a known magnitude. From equation (2.2), having a constant X and V_2 and knowing the value of V_1, the generator rotor angle δ_0 can be determined at steady state for a given P. V_2 is the voltage of the infinite bus and V_1 is the voltage at the sending end bus. Now assume a fault happens at the sending end bus. During the fault, the voltage of the bus is almost zero. However, the series controller tries to keep the P constant. As a result, it increases the quadrature component of the injected voltage. Therefore, with a constant X and V_2 when V_1 drops during the fault, δ increases to maintain the P constant. Now if V_1 returns back to its pre-fault value after clearing the fault, the generator also goes back to its pre-fault rotor angle δ_0 after some oscillations depending on the damping of the system. It is worth mentioning that if there is no change in the topology of the system and/or to the voltage magnitude, the generator must go back to pre-fault rotor angle. If there is a change in the system, or the voltage goes to a new steady state as a result of the controller response, the generator angle (δ) also goes to a new steady state after clearing the fault which is different from the pre-fault steady state.

When the fault is at the end of the transmission line and close to the infinite bus, and assuming that the P, Q controller is functioning properly, P and X are constant. Although the fault happens at V_2, the magnitude of V_2 does not drop much because it is connected to a very strong system and so it can be considered as constant. The same situation as what was explained for a fault at the sending bus of the UPFC, governs for a fault at the end of the line. Therefore, it can be said that the system remains stable if the post fault value for V_1 is the same as its pre-fault value or if it is different, it has an acceptable value. Otherwise, if voltage at the generator bus increases to some large value, the generator speed will drop and go out of synchronism eventually.

2.2.2 System with voltage control mode for UPFC

Figure (2.5) shows the voltage control mode for UPFC which is built in PSCAD. In this model, a voltage is injected directly to the line and therefore changes the power flow in the line.

As in section (2.2.1), this section will contain the explanations of the equal-area criterion for voltage control mode when a fault happens at either ends of the UPFC.

Figure (2.6) demonstrates the $P - \delta$ curve when a fault happens at the sending end of the UPFC. According to the curve, at steady state when $P_m = P_e$, the rotor angle is equal to δ_0. When a fault happens, the system goes through some transients and the machine speed will change and affect the rotor angle. In this case, when the fault occures at the sending end bus for a short period, the bus voltage becomes almost zero. Therefore, there is no power transfer between the generator and the infinite bus. Hence, the mechanical power input to the machine, which remained unchanged, is higher than the electrical power output during the fault and the machine speeds up. After the fault is cleared, there is no change in the topology of the system and the voltages at either ends have recovered and are back to their previous values. So, the $P - \delta$ curve for post fault condition is the same as pre fault curve. As was explained previously, during the fault the machine gains kinetic energy and the rotor angle increases. At the instatnt of clearing the fault, the rotor speed is higher than the synchronous speed so the rotor angle keeps going up until the machine loses all the kinetic energy it gained during the fault. At this time, rotor speed is the same as the synchronous speed, but P_e is larger than P_m. Therefore, the machine starts decelerating and rotor angle goes back toward its initial value, resulting in oscillations. If there is sufficient damping, the machine will eventually reach the steady state after some oscillations.

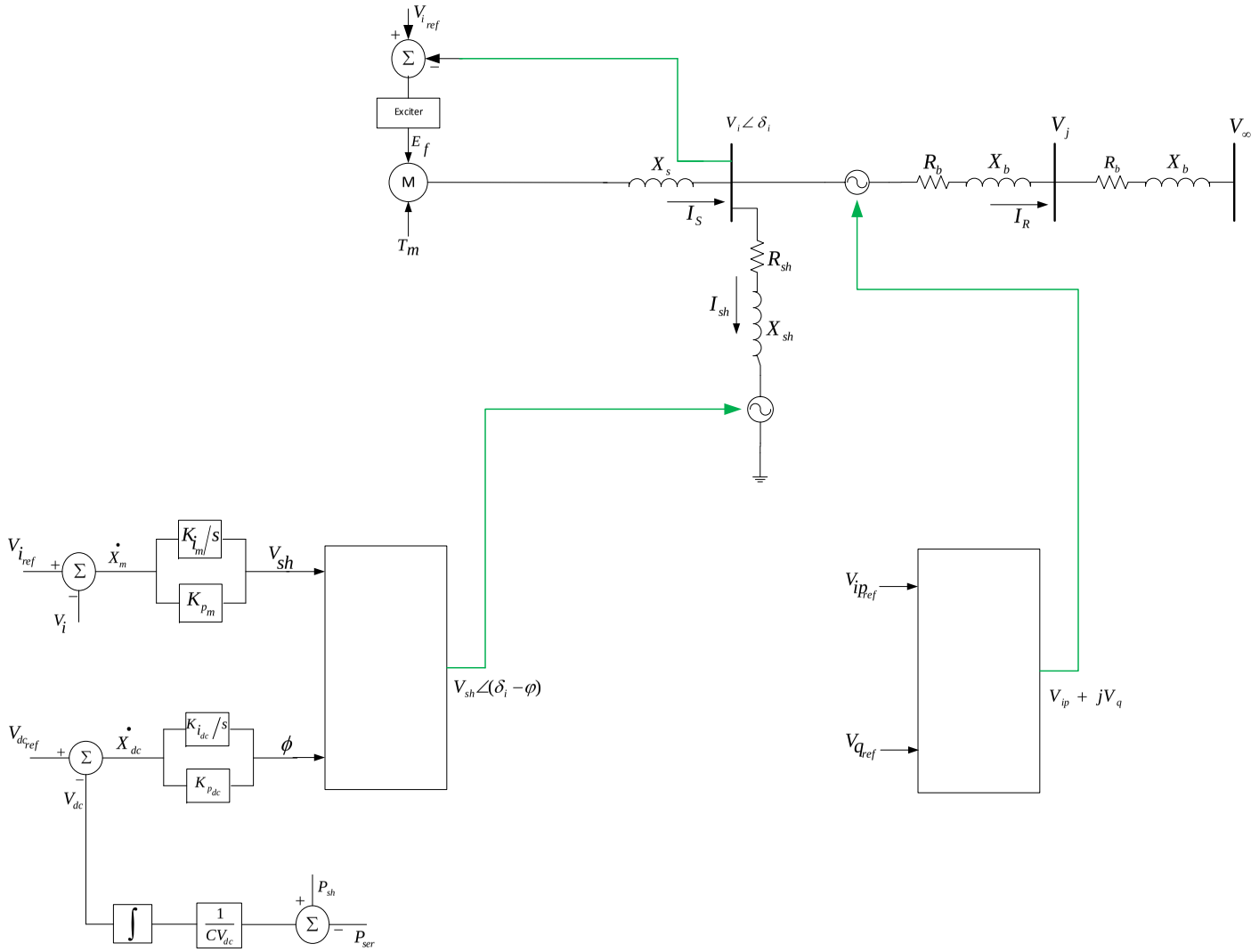

Figure 2.5: UPFC voltage control mode model including control parameters

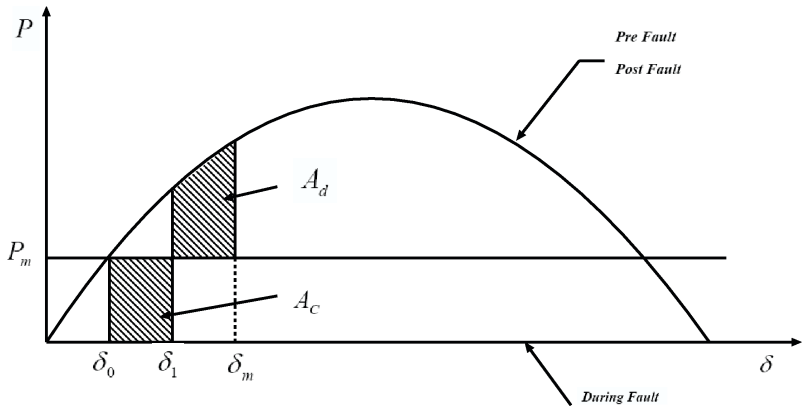

Figure 2.6: Equal-area criteria for the voltage control mode of UPFC for a fault at the sending bus

The transient response of the voltage control mode of the UPFC for a fault at the end of the transmission line and close to the infinite bus can be explained using the $P - \delta$ curve in figure (2.7). The $P - \delta$ curves for pre, during, and post fault situations for the model are shown in this figure. The power angle relationship for post and pre fault conditions are the same for a fault at the end of the transmission line and close to the infinite bus. As a result of that, the decelerating area is equal to the accelerating area and the machine remains stable. It can be figured out from the equal-area criterion that the voltage control mode behaves more robustly for faults at either ends of the UPFC.

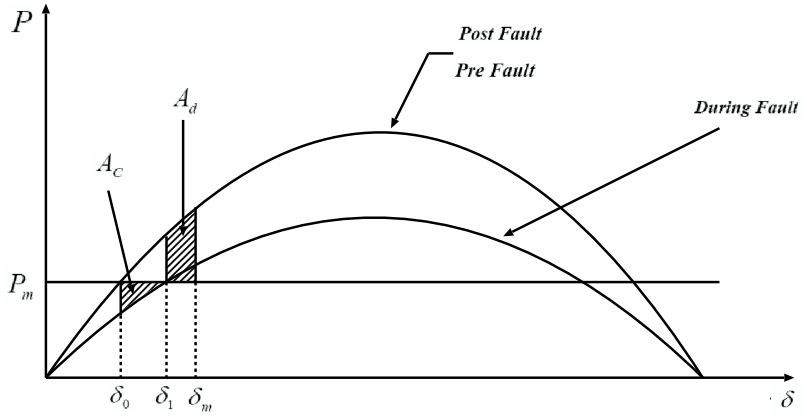

Figure 2.7: Equal-area criteria for the voltage control mode of UPFC for a fault at the infinite bus

2.3 Comparison between two UPFC models

For the purpose of comparison of the two modes, only a small disturbance is applied. Because the goal of the thesis is to investigate the response of the two modes of operation to small disturbances.

In order to give a small disturbance, the mechanical torque on the shaft is increased by a 1 % pulse. The duration of the pulse in 100 ms.

Figure (2.8) shows the machine rotor angle. The change to the T_m is applied at 25 s. As it can be observed from this figure, when the machine torque is increased the machine angle keeps increasing for the P, Q control mode. However, in the case of the voltage control mode, the machine angle is able to return back to its pre-disturbance value after the disturbance is cleared. Therefore, it can be conducted that the P, Q control mode is unstable. The reason can be explained in this way. Before applying any disturbance, the mechanical power input of the machine is the same as the electrical power output. The mechanical output of the machine increases as a result of increasing the machine torque. In the case of the P, Q control mode, the series controller tries to keep the electrical power at the reference value. Therefore, after the disturbance, the mechanical power is larger than the electrical power. Since the electrical power is kept constant, the machine cannot get rid of the extra energy it gains because of the increment in T_m. As a result, it becomes unstable.

On the other hand, with the voltage control mode, since there is no active power controller, the machine releases the extra energy to the transmission line and therefore stays stable.

Figure (2.9) shows the active power flow in the line for both modes of control. According to this figure, the P, Q control mode tries to tide up the active power flow in the line. Therefore, it has a smaller oscillation comparing to the voltage control mode. However, the voltage control mode shows a larger oscillation because the generator is injecting more active power flow to the line.

Figures (2.10) and (2.11) show the in-phase and quadrature components of the series

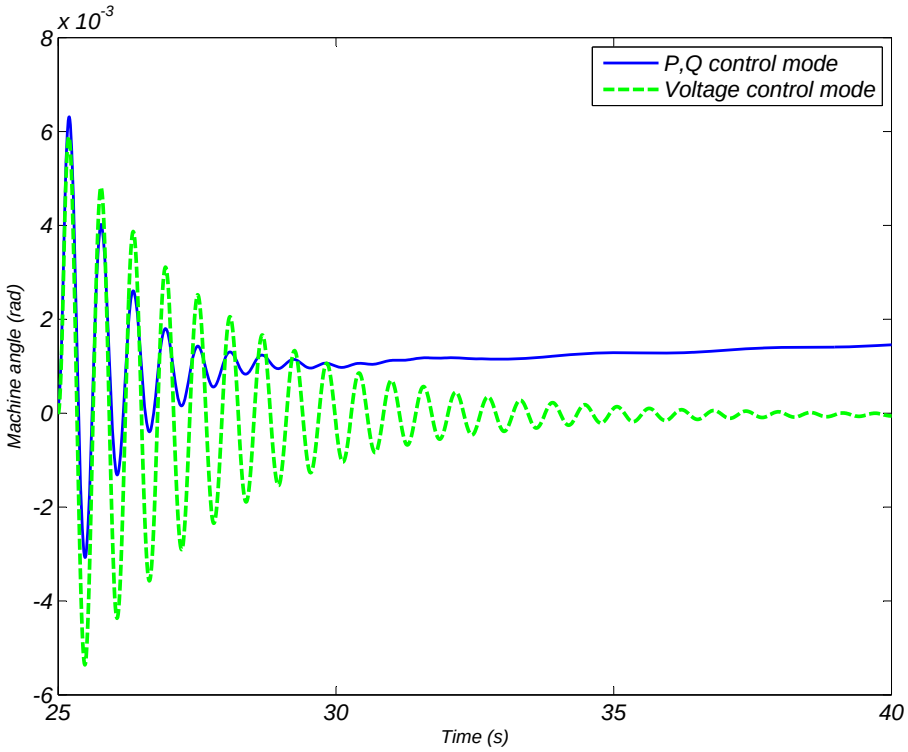

Figure 2.8: Machine angle for a pulse change in the machine torque (T_m)

injected voltage respectively.

From the comparisons presented in this chapter it can be concluded that if a small disturbance is applied to the machine torque, the P, Q control mode goes out of synchronism and becomes unstable. It shows the need to develop the small signal stability model of the voltage control mode for UPFC.

This chapter covered the concepts of transient stability in power systems and the method that could be used to predict the stability of a system. In this chapter, two proposed models for UPFC were compared from transient stability point of view. This chapter confirmed the necessity of having two control modes for UPFC by showing a case in which the voltage control mode shows a better performance than the power control mode. The next two chapters are devoted to development of these models. Chapter (3) presents the modeling of the shunt branch of the UPFC (i.e. STATCOM). Chapter (4) presents the small signal stability model of UPFC for both modes of control.

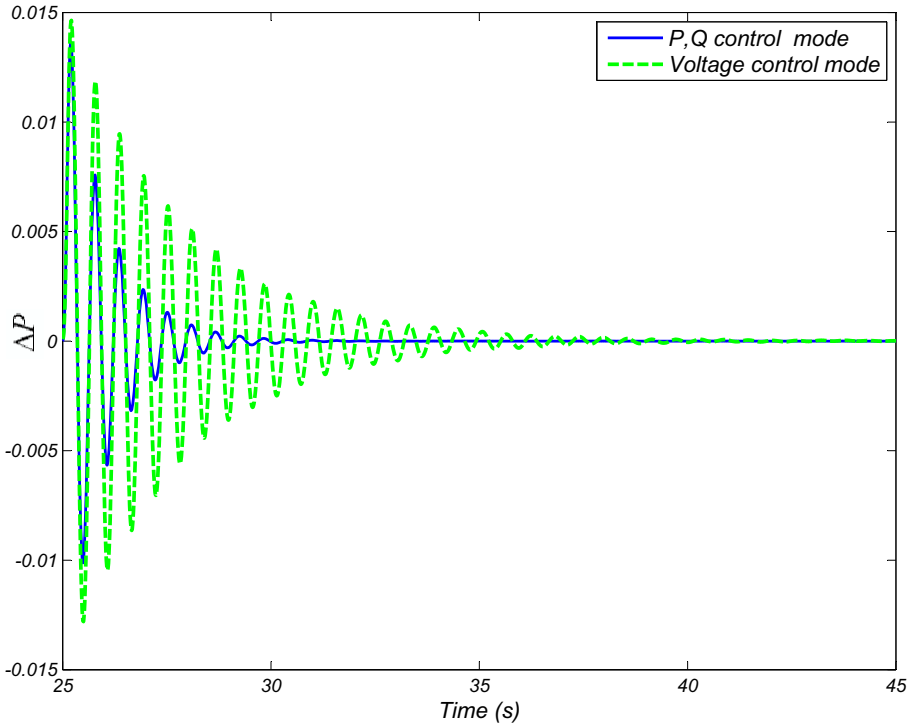

Figure 2.9: Active power flow in the line for a pulse change in the machine torque (T_m)

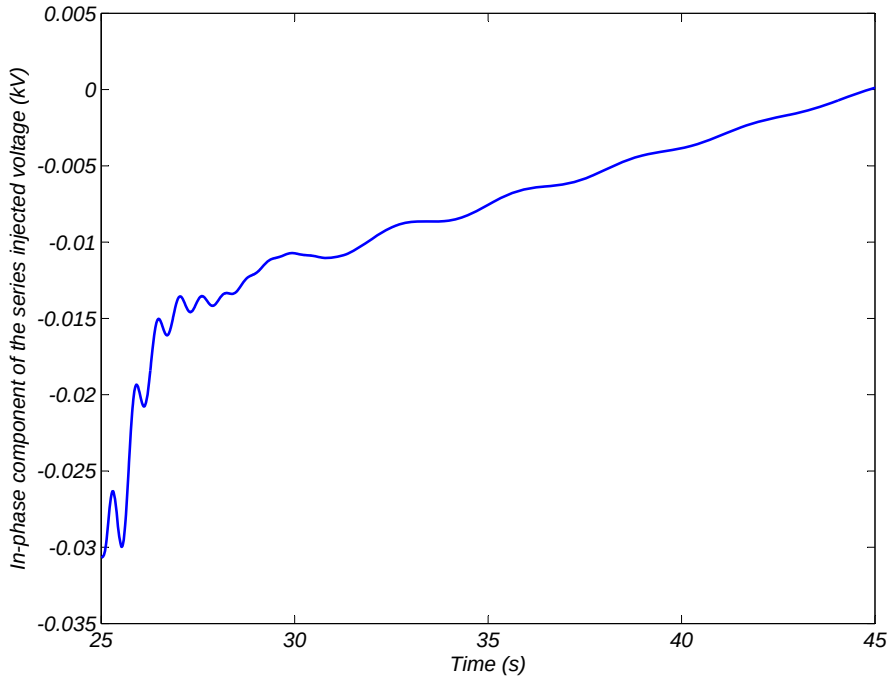

Figure 2.10: In-phase component of the series injected voltage for a pulse change in the machine torque (T_m)

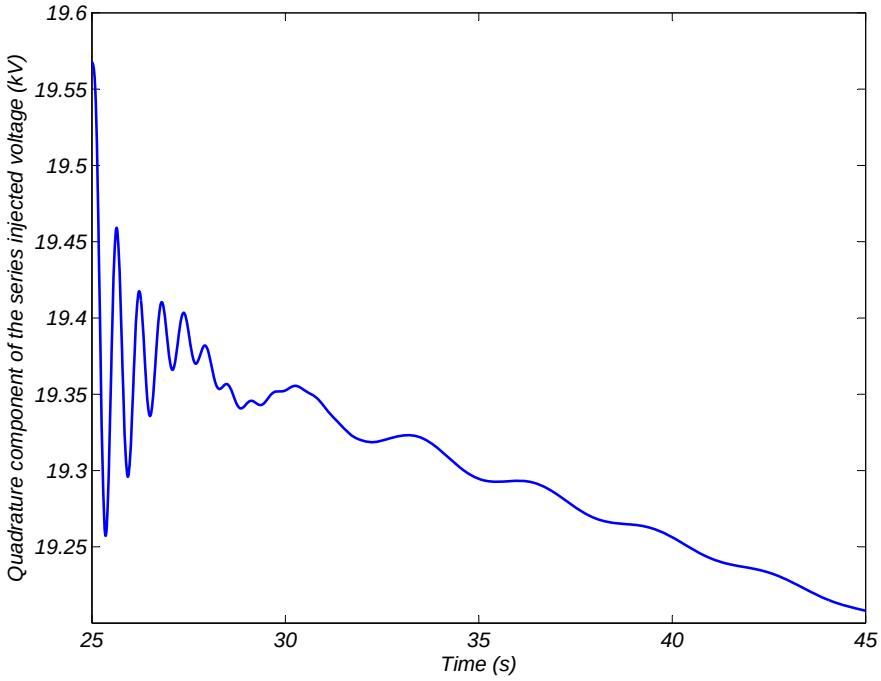

Figure 2.11: Quadrature component of the series injected voltage for a pulse change in the machine torque (T_m)

3 STATCOM Small Signal Model

3.1 STATCOM Small Signal Equations with constant Admittance Matrix Model for the Network

This section gives the details of how to derive the small signal stability model of a STATCOM when the remaining network is modeled with constant admittance matrix. To have a better understanding of how to proceed during the steps of modeling, a simple three bus system is used as is shown in figure (3.1). A STATCOM is connected to the middle bus V_i. V_3 is modeled as an infinite bus and V_1 is a voltage controlled (PV) bus. The idea is to keep V_i constant at a reference value using the STATCOM connected to the bus.

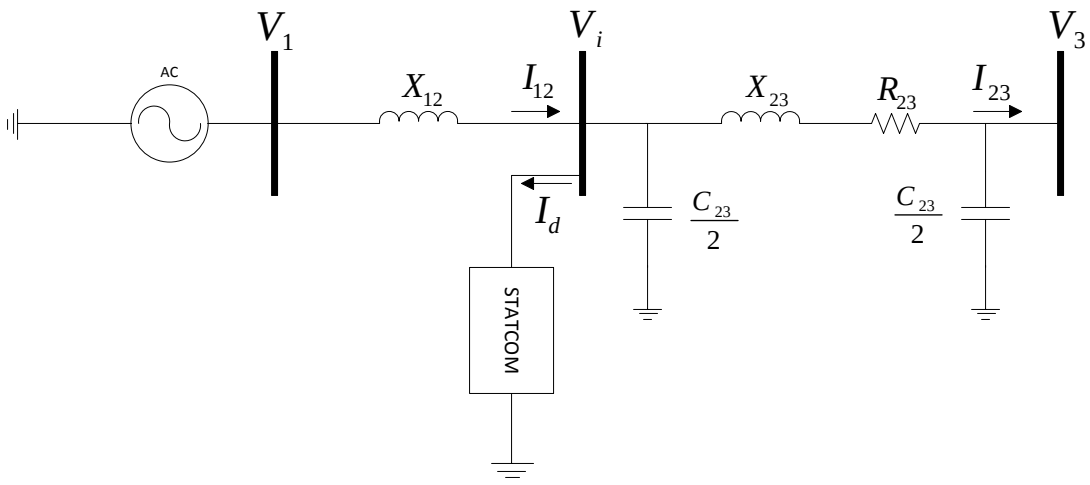

Figure 3.1: A simple test system with STATCOM connected to it

In order to derive matrix equations, the algebraic and state equations are to be written and then linearized around the operating point. The algebraic and state equations are given in equations (3.1) to (3.6) and (3.7) to (3.9) respectively.

In equation (3.1), V_{sh_x} is the real component, i.e. x-component, of V_{sh}. V_{sh} itself is the magnitude of the shunt voltage injected to the bus that the STATCOM is connected to. δ_i is the phase angle of the bus voltage where the STATCOM is connected to the network. In

the derivations presented here, δ_i is considered to be the phase reference of the network. ϕ is the phase difference between reference angle (δ_i) and shunt injected voltage angle (δ_{sh}).

$$V_{sh_x} = V_{sh}cos(\delta_i - \phi) \Rightarrow$$
$$\Delta V_{sh_x} = cos(\delta_i - \phi)\Delta V_{sh} - V_{sh}sin(\delta_i - \phi)\Delta\delta_i + V_{sh}sin(\delta_i - \phi)\Delta\phi \tag{3.1}$$

The phasor diagram for the voltages is shown in figure (3.2).

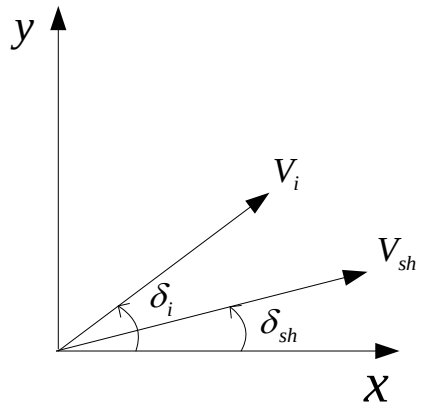

Figure 3.2: Phasor diagram for STATCOM voltages

V_{sh_y} is the imaginary component, i.e. y-component, of V_{sh}. V_{sh}, δ_i, and ϕ are already defined.

$$V_{sh_y} = V_{sh}sin(\delta_i - \phi) \Rightarrow$$
$$\Delta V_{sh_y} = sin(\delta_i - \phi)\Delta V_{sh} + V_{sh}cos(\delta_i - \phi)\Delta\delta_i - V_{sh}cos(\delta_i - \phi)\Delta\phi \tag{3.2}$$

The magnitude of the shunt injected voltge is controlled using a PI controller. The block diagram including the PI controller is shown in figure (3.3). $V_{i_{ref}}$ is the desired voltage of the bus that the STATCOM is connected to. V_i is the voltage magnitude of the same bus.

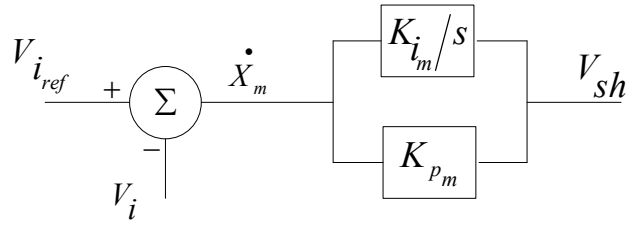

Figure 3.3: PI controller for the shunt injected voltage

$$V_{sh} = K_{i_m} X_m + \left(V_{i_{ref}} - V_i\right) K_{p_m} \Rightarrow$$
$$\Delta V_{sh} = K_{i_m} \Delta X_m + K_{p_m} \left(\Delta V_{i_{ref}} - \Delta V_i\right) \tag{3.3}$$

ϕ is the output of the PI controller which controls the voltage across the DC capacitor in STATCOM. The corresponding PI controller is drawn in figure (3.4).

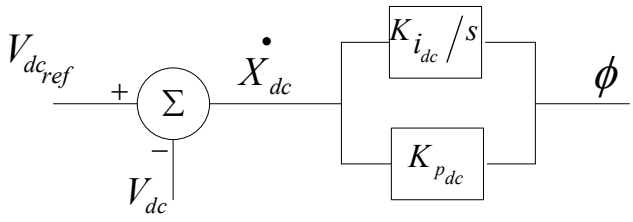

Figure 3.4: PI controller for DC voltage across the capacitor

$$\phi = K_{i_{dc}} X_{dc} + \left(V_{dc_{ref}} - V_{dc}\right) K_{p_{dc}} \Rightarrow$$
$$\Delta\phi = K_{i_{dc}} \Delta X_{dc} + K_{p_{dc}} \left(\Delta V_{dc_{ref}} - \Delta V_{dc}\right) \tag{3.4}$$

As already explained, δ_i is the phase angle of the bus voltage where the STATCOM is connected to the rest of the network through that bus. If the x and y compenents of the bus voltage are known, the angle can be easily calculated using equation (3.5).

$$tan(\delta_i) = \frac{V_{i_y}}{V_{i_x}} \Rightarrow$$
$$sec^2\delta_i \Delta\delta_i = -\frac{V_{i_y}}{V_{i_x}^2} \Delta V_{i_x} + \frac{1}{V_{i_x}} \Delta V_{i_y} \tag{3.5}$$

As mentioned previously, V_i is the magnitude of the bus voltage with STATCOM connected to the bus. Equation (3.6) can be used to calculate V_i from V_{i_x} and V_{i_y}.

$$V_i = \sqrt{V_{i_x}^2 + V_{i_y}^2} \Rightarrow$$
$$\Delta V_i = \frac{V_{i_x}}{|V_i|} \Delta V_{i_x} + \frac{V_{i_y}}{|V_i|} \Delta V_{i_y} \tag{3.6}$$

After the steady state equations are defined it is time to introduce the state and current injection eqution. Every dynamic device is defined with a set of state and current injection equations. The corresponding state and current equations for the STATCOM is given in the following sets of formulas.

The STATCOM model can be completely defined by three state variables. The derivative of the first state variable is defined as $\dot{X}_{dc}$ according to equation (3.7). It is the output of the summation block in the figure (3.4).

$$\begin{aligned}
&\dot{X}_{dc} = \left(V_{dc_{ref}} - V_{dc}\right) \Rightarrow \\
&\Delta\, \dot{X}_{dc} = \left(\Delta V_{dc_{ref}} - \Delta V_{dc}\right)
\end{aligned} \tag{3.7}$$

The second state variable that is used to define the STATCOM model is X_m. The deravative of this state variable, i.e. $\dot{X}_m$, is the output of the summation block in figure (3.3).

$$\begin{aligned}
&\dot{X}_{m} = \left(V_{i_{ref}} - V_{i}\right) \Rightarrow \\
&\Delta\, \dot{X}_{m} = \left(\Delta V_{i_{ref}} - \Delta V_{i}\right)
\end{aligned} \tag{3.8}$$

Finally the third state variable is the DC voltage across the capacitor. Equation (3.9) is actually the power balance equation across the capacitor. Since all other equations are in p.u., this equation has also been converted to p.u. values. $Index_{dc}$ is the converting coefficient between the actual and p.u. formula and is equal to $Index_{dc} = CV_{dc}^2/S_b$. Note that all the equations are in p.u. except for $Index_{dc}$ where C, V_{dc} and S_b are in their actual values. . P_{sh} is the active power flow exchange between STATCOM and the network.

$$\begin{aligned}
&\dot{V}_{dc} = \frac{P_{sh}}{Index_{dc} V_{dc}}) \Rightarrow \\
&\Delta\, \dot{V}_{dc} = \frac{\Delta P_{sh}}{Index_{dc} V_{dc}} - \frac{P_{sh} \Delta V_{dc}}{Index_{dc} V_{dc}^2}
\end{aligned} \tag{3.9}$$

Equation (3.10) shows the current that is absorbed from the network by the STATCOM. $(g_{sh} + jb_{sh})$ is the admittance of the exciter transformer that connects STATCOM to the network.

$$\begin{aligned}
I_{sh_x} + jI_{sh_y} &= \left(V_{i_x} + jV_{i_y} - V_{sh_x} - jV_{sh_y}\right)(g_{sh} + jb_{sh}) \Rightarrow \\
\Delta I_{sh_x} + j\Delta I_{sh_y} &= (g_{sh} + jb_{sh})\,\Delta V_{i_x} + (-b_{sh} + jg_{sh})\,\Delta V_{i_y} \\
&\quad - (g_{sh} + jb_{sh})\,\Delta V_{sh_x} + (b_{sh} - jg_{sh})\,\Delta V_{sh_y}
\end{aligned} \tag{3.10}$$

Now, all the above equations can be written in a matrix format. The idea is to combine the equations so that the whole system can be written in the format of standard state

equations i.e. $\Delta \dot{X} = A\Delta X + B\Delta U$.

If the linearized steady state equations, i.e. equation (3.1) to (3.6) are put together in a matrix format, the result is equation (3.11). In this equation, ΔZ is a set of intermediate variables; ΔX is the set of state equations; ΔU defines the inputs to the model and ΔV includes the voltage of the bus with STATCOM connected to it.

$$F\Delta Z + G\Delta X + K\Delta U + H\Delta V = 0 \tag{3.11}$$

In the same way, if the linearized state equations, equations (3.7)-(3.9), are combined together in a matrix format, it results in equation (3.12).

$$\Delta \dot{X} = L\Delta X + M\Delta U + P\Delta V + N\Delta Z \tag{3.12}$$

Equation (3.13) is in fact the current injection equation (equation (3.10)), when it is written in matrix form. It should be mentioned that the last three equations were organized to be written as a function of ΔX, ΔU, ΔV, and ΔZ.

$$\Delta I_{sh} = Y_{sh}\Delta V - I_2\Delta Z \tag{3.13}$$

Each of the matrices in equations (3.11), (3.12) and (3.13) are defined below. As it was explained earlier, the goal is to describe the STATCOM model in the standard state space format. To do so, ΔZ can be calculated as a function of ΔX, ΔU and ΔV from equation (3.11). Then, ΔZ is replaced in (3.12) and (3.13) to write $\Delta \dot{X}$ and ΔI_{sh} as a function of ΔX, ΔU and ΔV, resulting in the final state and current equations for the dynamic device (equation (3.15)).

$$\Delta Z = -F^{-1}G\Delta X - F^{-1}K\Delta U - F^{-1}H\Delta V \tag{3.14}$$

$$\Delta \dot{X}_d = A_d\Delta X_d + B_d\Delta U_d + E_d\Delta V$$
$$\Delta I_d = C_d\Delta X_d + D_d\Delta U_d + Y_d\Delta V \tag{3.15}$$

$$A_d = \left(L - NF^{-1}G\right) \qquad B_d = \left(M - NF^{-1}K\right) \qquad E_d = \left(P - NF^{-1}H\right)$$

$$C_d = \left(I_2F^{-1}G\right) \qquad D_d = \left(I_2F^{-1}K\right) \qquad Y_d = \left(Y_{sh} + I_2F^{-1}H\right)$$

By equating the current injection from network ($\Delta I_N = Y_N \Delta V$) and the device current from equation (3.15), ΔV can be derived as a function of ΔX and ΔU as in (3.16).

$$\Delta V = -\left(Y_N + Y_d\right)^{-1} C_d \Delta X_d - \left(Y_N + Y_d\right)^{-1} D_d \Delta U_d \tag{3.16}$$

Therefore, the final state equation for the whole system can be written by replacing ΔV from equation (3.16) in (3.15). The final state equation representing the system including the STATCOM, is given in (3.17) and is used to determine the stability of the system.

$$\Delta \dot{X}_{sys} = A_{sys}\Delta X_{sys} + B_{sys}\Delta U_{sys} \tag{3.17}$$

$$A_{sys} = A_d - E_d\left(Y_N + Y_d\right)^{-1} C_d \qquad B_{sys} = B_d - E_d\left(Y_N + Y_d\right)^{-1} D_d$$

$$\Delta Z = \begin{bmatrix} \Delta V_{sh_x} \\ \Delta V_{sh_y} \\ \Delta V_{sh} \\ \Delta \phi \\ \Delta \delta_i \\ \Delta |V_i| \end{bmatrix} \quad \Delta X = \begin{bmatrix} \Delta X_{dc} \\ \Delta X_m \\ \Delta V_{dc} \end{bmatrix} \quad \Delta U = \begin{bmatrix} \Delta V_{dc_{ref}} \\ \Delta V_{i_{ref}} \end{bmatrix} \quad \Delta V = \begin{bmatrix} \Delta V_{i_x} \\ \Delta V_{i_y} \end{bmatrix}$$

$$F = \begin{bmatrix} -1 & 0 & cos(\delta_i - \phi) & V_{sh}sin(\delta_i - \phi) & -V_{sh}sin(\delta_i - \phi) & 0 \\ 0 & -1 & sin(\delta_i - \phi) & -V_{sh}cos(\delta_i - \phi) & V_{sh}cos(\delta_i - \phi) & 0 \\ 0 & 0 & -1 & 0 & 0 & -K_{pm} \\ 0 & 0 & 0 & -1 & 0 & 0 \\ 0 & 0 & 0 & 0 & -sec^2(\delta_i) & 0 \\ 0 & 0 & 0 & 0 & 0 & -1 \end{bmatrix}$$

$$G = \begin{bmatrix} 0 & 0 & 0 \\ 0 & 0 & 0 \\ 0 & K_{i_m} & 0 \\ K_{i_{dc}} & 0 & -K_{p_{dc}} \\ 0 & 0 & 0 \\ 0 & 0 & 0 \end{bmatrix} \quad H = \begin{bmatrix} 0 & 0 \\ 0 & 0 \\ 0 & 0 \\ 0 & 0 \\ \frac{-V_{i_y}}{V_{ix}^2} & \frac{1}{V_{i_x}} \\ \frac{V_{i_x}}{|V_i|} & \frac{V_{i_y}}{|V_i|} \end{bmatrix} \quad K = \begin{bmatrix} 0 & 0 \\ 0 & 0 \\ 0 & K_{p_m} \\ K_{p_{dc}} & 0 \\ 0 & 0 \\ 0 & 0 \end{bmatrix}$$

$$L = \begin{bmatrix} 0 & 0 & -1 \\ 0 & 0 & 0 \\ 0 & 0 & -\frac{P_{sh}}{Index_{dc}V_{dc}^2} \end{bmatrix} \quad M = \begin{bmatrix} 1 & 0 \\ 0 & 1 \\ 0 & 0 \end{bmatrix} \quad P = \begin{bmatrix} 0 & 0 \\ 0 & 0 \\ \frac{k_3}{Index_{dc}V_{dc}} & \frac{k_4}{Index_{dc}V_{dc}} \end{bmatrix}$$

$$N = \begin{bmatrix} 0 & 0 & 0 & 0 & 0 & 0 \\ 0 & 0 & 0 & 0 & 0 & -1 \\ \frac{k_1}{Index_{dc}V_{dc}} & \frac{k_2}{Index_{dc}V_{dc}} & 0 & 0 & 0 & 0 \end{bmatrix} \quad I_2 = \begin{bmatrix} g_{sh} & -b_{sh} & 0 & 0 & 0 & 0 \\ b_{sh} & g_{sh} & 0 & 0 & 0 & 0 \end{bmatrix}$$

$$Y_{sh} = \begin{bmatrix} g_{sh} & -b_{sh} \\ b_{sh} & g_{sh} \end{bmatrix} \qquad Y_N = \begin{bmatrix} g_{22} & -b_{22} \\ b_{22} & g_{22} \end{bmatrix}$$

k_1, k_2, k_3 and k_4 are coefficients of ΔV_{sh_x}, ΔV_{sh_y}, ΔV_{i_x} and ΔV_{i_y} respectively in the linearzied formula of ΔP_{sh} and are defined in the following equations.

$$k_1 = g_{sh}V_{i_x} - b_{sh}V_{i_y} - g_{sh}V_{sh_x} + b_{sh}V_{sh_y} - g_{sh}V_{sh_x} - b_{sh}V_{sh_y}$$

$$k_2 = b_{sh}V_{i_x} + g_{sh}V_{i_y} - b_{sh}V_{sh_x} - g_{sh}V_{sh_y} + b_{sh}V_{sh_x} - g_{sh}V_{sh_y}$$

$$k_3 = g_{sh}V_{sh_x} + b_{sh}V_{sh_y}$$

$$k_4 = -b_{sh}V_{sh_x} + g_{sh}V_{sh_y}$$

A power network can be described completely by its admittance matrix which is known as Y-bus. g_{22} and b_{22} are elements of the network Y-bus for the system shown in figure (3.1).

$$g_{22} = Real\left(\frac{1}{Z_{12}} + \frac{1}{Z_{23}}\right)$$

$$b_{22} = Imag\left(\frac{1}{Z_{12}} + \frac{1}{Z_{23}}\right)$$

3.2 Validation of STATCOM small signal model against PSCAD

Figure (3.5) shows the STATCOM model which is built in PSCAD. The model is used to validate the small signal stability (SSS) model. PSCAD is a strong and accurate tool for studying dynamic behaviors of any types of power systems. According to figure (3.5), the STATCOM is modeled using a voltage source and an impedance.

A PI controller controls the AC bus voltage by taking the voltage at the bus and comparing it to a reference value. Based on the difference between the measured and reference value, it injects or absorbs reactive power to maintain the voltage at the reference value.

When a STATCOM is connected to a network, it is only the reactive power flow which is exchanged between the STATCOM and the network. Active power exchange between

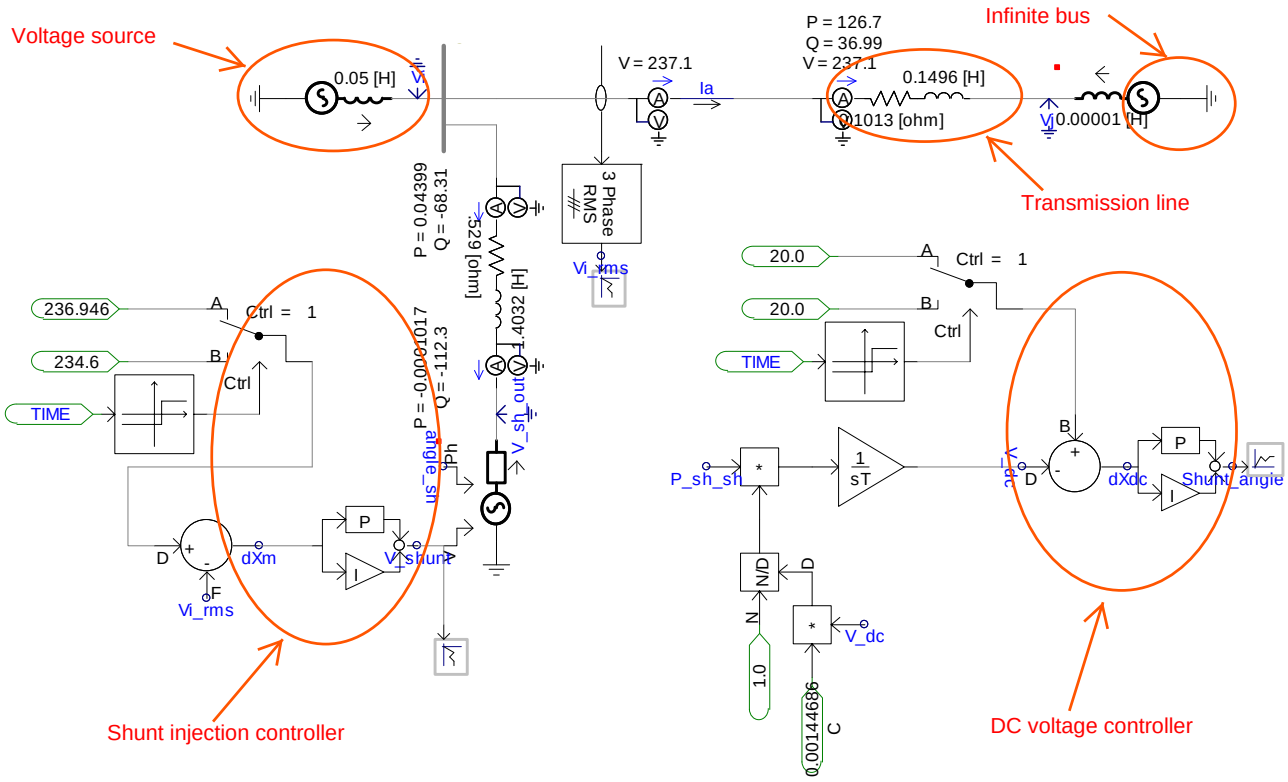

Figure 3.5: STATCOM model in PSCAD

the two buses is zero in an ideal system with no losses. Therefore, the shunt voltage angle is equal to the AC voltage angle.

3.2.1 Comparison of SSS model with PSCAD for a change in reference value of AC bus voltage

As explained before in section (1.2), if the disturbance applied to a system is small enough, the nonlinear system can be linearized around the operating point, and the dynamic response can be simulated using the linear model. The same approach has been taken here to validate the SSS model. The nonlinear system in PSCAD has been linearized around the steady state point, resulting in a SSS model. Consequently, the SSS model is expected to show the same transient behavior as the nonlinear model for a small disturbance.

This section presents the waveforms for both the SSS model and PSCAD when the reference value of AC voltage has increased by 1 %. Figure (3.6) shows the AC bus voltage;

the SSS model behaves exactly the same as the PSCAD model.

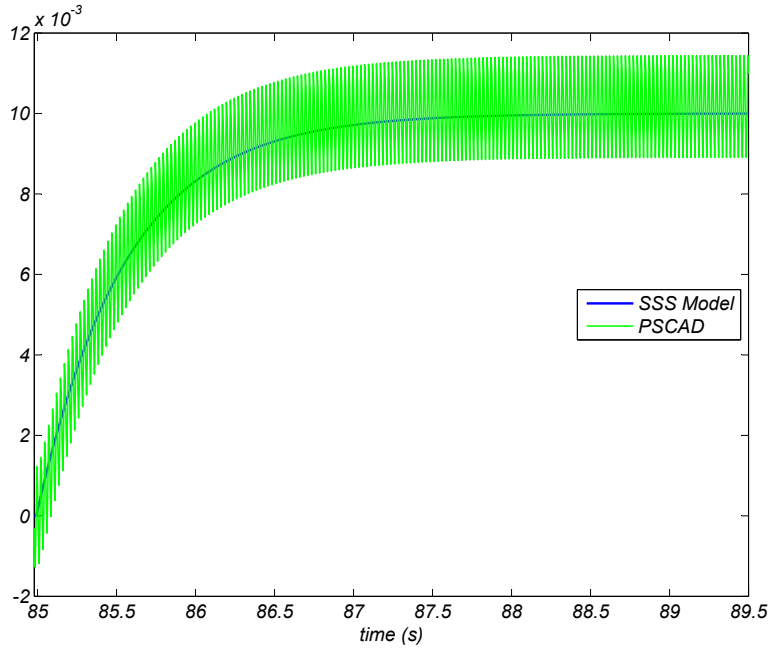

Figure 3.6: ΔV_i for a change in the reference value of V_i

Figure (3.7) shows the state variable X_m for both models. $\dot{X_m}$ is in fact the voltage error signal; i.e. $\dot{X_m} = V_{i_{ref}} - V_i$. The blue line is the SSS model and the green one is the PSCAD model. The two curves are close to each other in this figure. Figures (3.8) and (3.9) show the active and reactive power flows in the line respectively. According to these figures the SSS model is pretty close to the PSCAD model.

3.2.2 Comparison of the SSS model with PSCAD for a change in reference value of the DC bus voltage

In the previous section, the SSS model was compared against the PSCAD model for a change in the reference value of the AC bus voltage. In this section, the two models are compared for a variation in the reference value of the DC bus voltage by 5 %. Figure (3.10) includes the DC bus voltage which is one of the state variables in the system. According to this figure, the SSS model is close to the PSCAD model. Figure (3.11) shows another state variable in the system, X_{dc}. From figure (3.11), the SSS model has the same frequency as

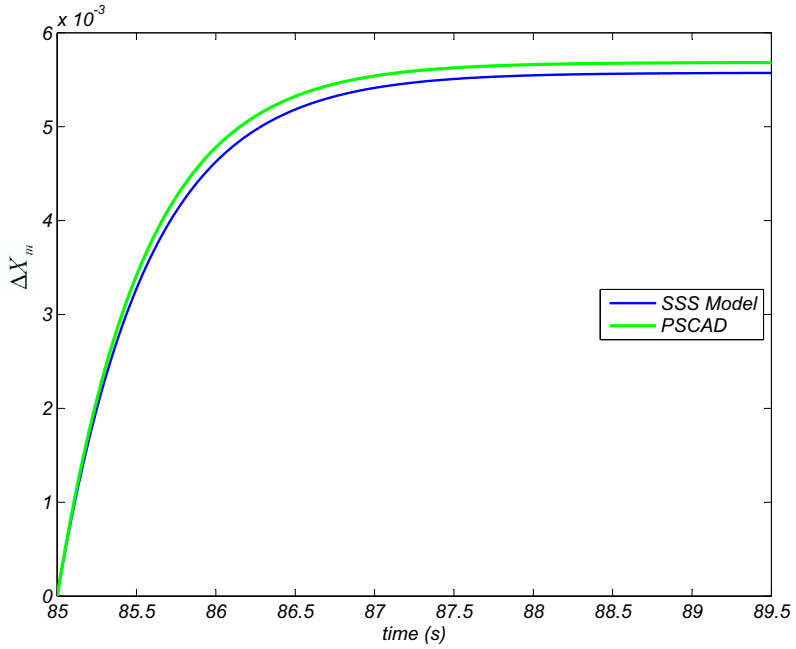

Figure 3.7: ΔX_m for a change in the reference value of V_i

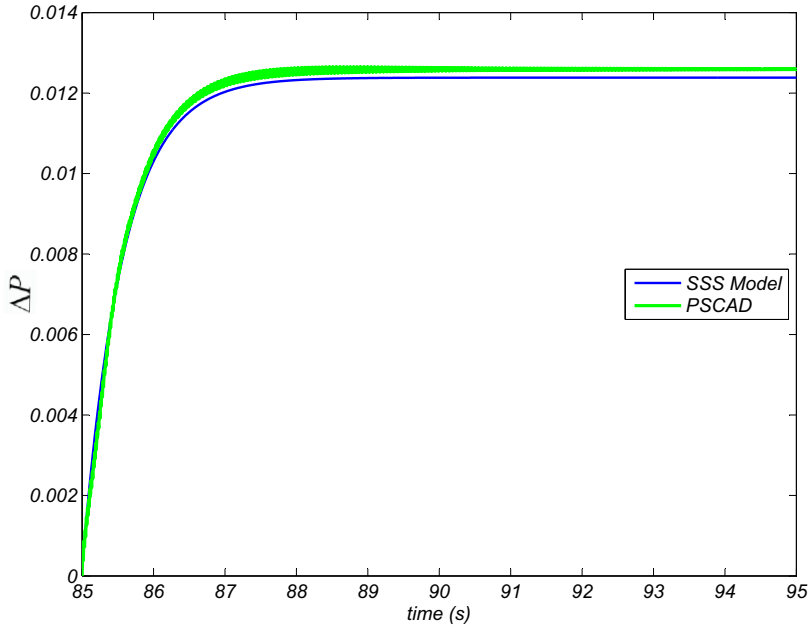

Figure 3.8: ΔP_{line} for a change in the reference value of V_i

the PSCAD model although the amplitudes of the waveforms are a bit different from each other.

At the end of the comparison between the SSS model and the PSCAD model, figures

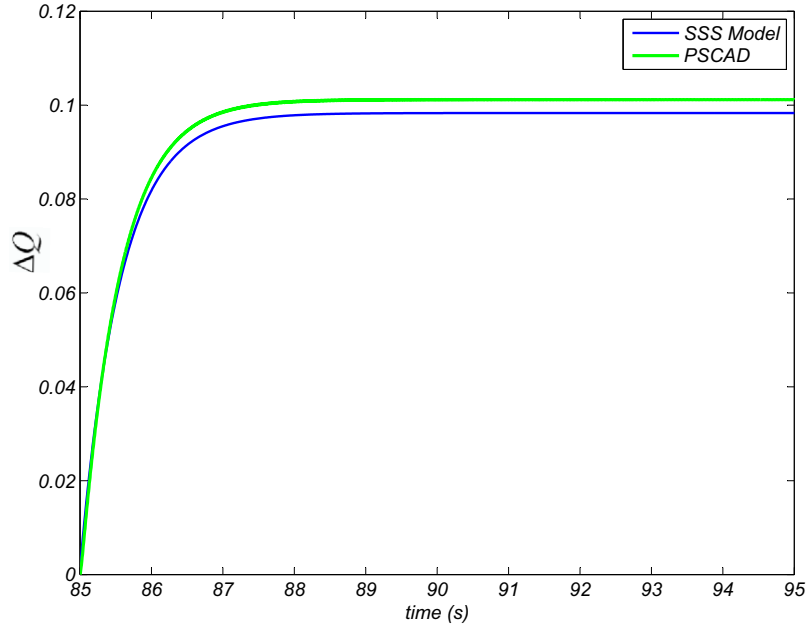

Figure 3.9: ΔQ_{line} for a change in the reference value of V_i

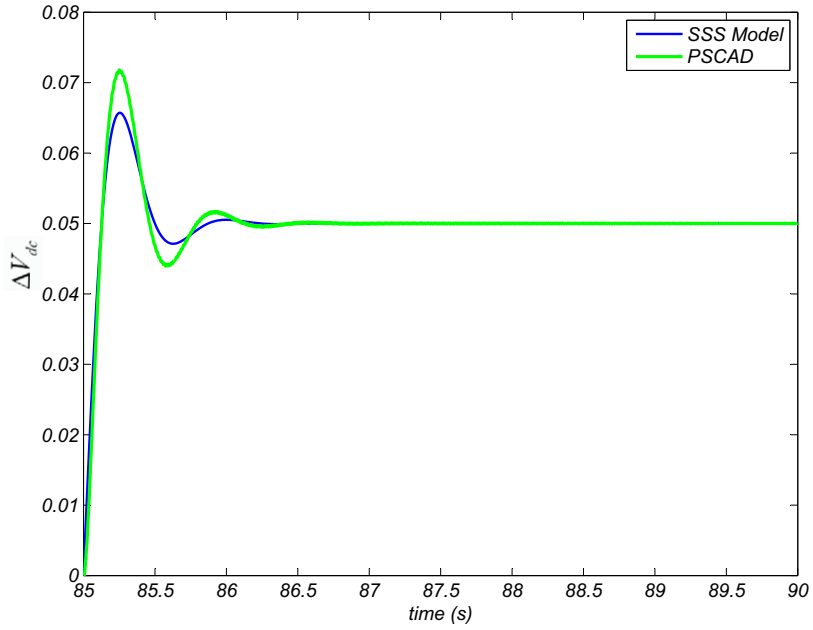

Figure 3.10: ΔV_{dc} for a change in the reference value of V_{dc}

(3.12) and (3.13) show the active and reactive power flows in the line. Based on these figures, for a change in $V_{dc_{ref}}$ P and Q in the line closely match in the SSS model with PSCAD.

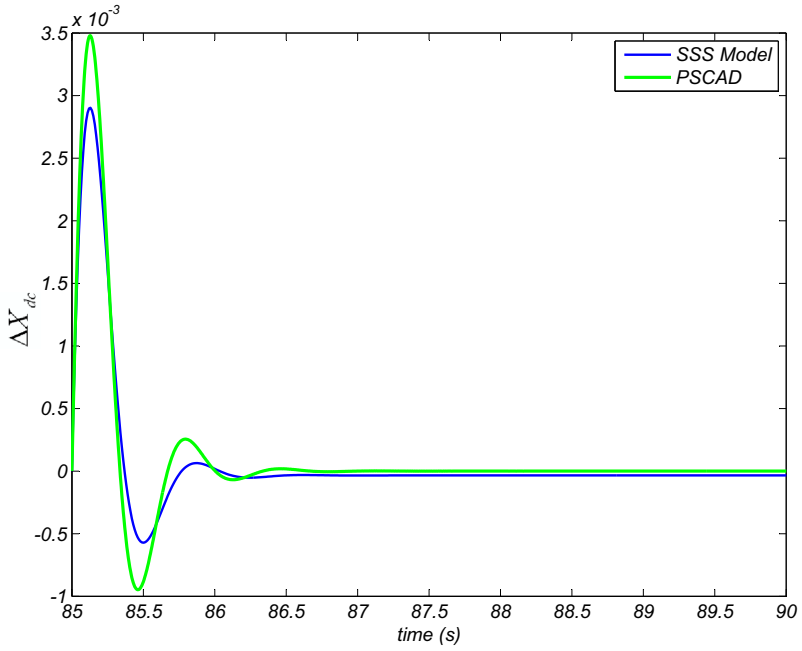

Figure 3.11: ΔX_{dc} for a change in the reference value of V_{dc}

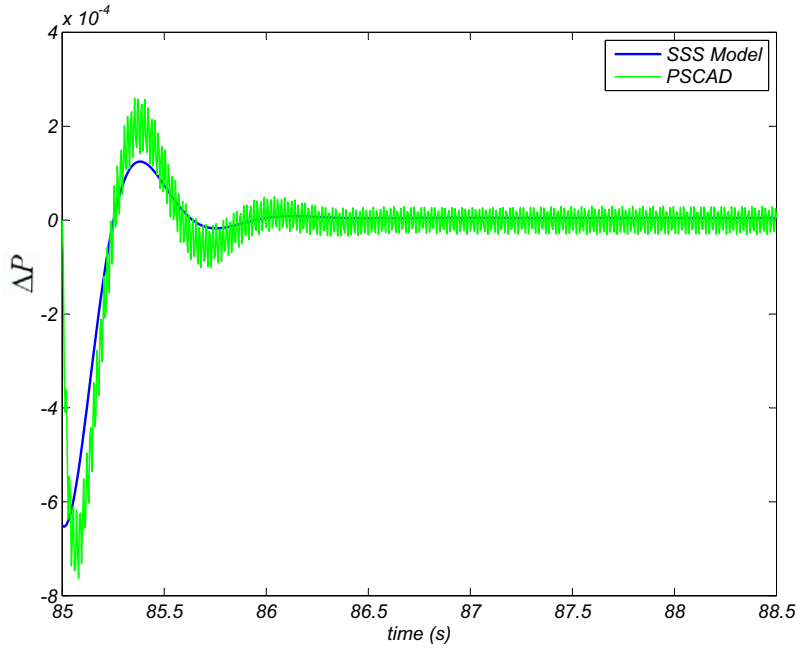

Figure 3.12: ΔP_{line} for a change in the reference value of V_{dc}

In conclusion, as reported by the comparisons in sections (3.2.1) and (3.2.2), the SSS model is following the transient model represented in PSCAD. Hence, the SSS model for

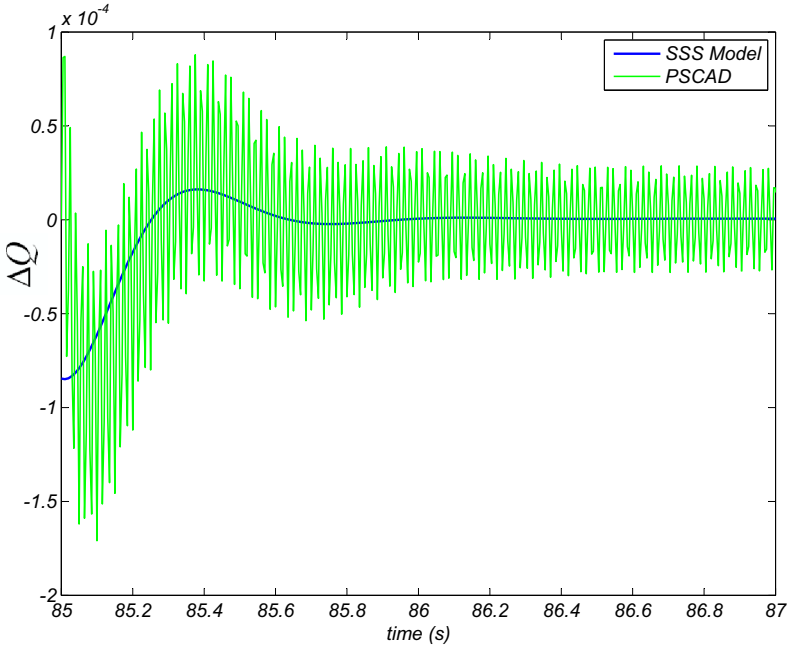

Figure 3.13: ΔQ_{line} for a change in the reference value of V_{dc}

STATCOM is validated.

4 UPFC Small Signal Model

UPFC is considered to be composed of one shunt and one series controller. The shunt controller is actually a STATCOM and the series controller is an SSSC. These two controllers are connected together through a DC capacitor to form a UPFC. Figure (4.1) shows the single line diagram of a system with a UPFC embedded in it. The bus V_i is the sending end bus and V_j is the receiving end bus. $(R_b + jX_b)$ is the booster transformer impedance and V_{ser} is the injected series voltage. $(R_{sh} + jX_{sh})$ is the exciter transformer impedance and V_{sh} models the AC voltage source in the shunt branch. I_S and I_R are the sending and receiving end currents respectively. The bus with label V_∞ represents a very strong system behind the bus, i.e. an infinite bus.

In the following parts of this chapter, the power control mode is validated against PSCAD while the voltage control mode is validated by solving nonlinear equations. An attempt was also done to validate the voltage control mode by PSCAD; however the results of PSCAD were not matching with the small signal stability model. Since the small signal stability model is satisfying the nonlinear equations, it can be concluded that the voltage control mode was not modeled correctly in PSCAD. It has been left as future works to develop voltage control mode in PSCAD and compare it with the small signal stability model.

4.1 Small Signal Stability Model of UPFC Power Control Mode

As it was explained in chapter (3), in order to derive the SSS model, we need to write a set of algebraic and state equations. The set of algebraic equations are steady state equations which govern the system. The state equations mostly come from the controllers in the system. Equations (4.1)-(4.12) are the set of algebraic equations needed to derive SSS model for UPFC power control mode. Equations (4.13) to (4.17) include the state equations. Four of the state equations come from the four PI controllers used to control the system parameters and one of them is the DC voltage across the DC capacitor in the UPFC.

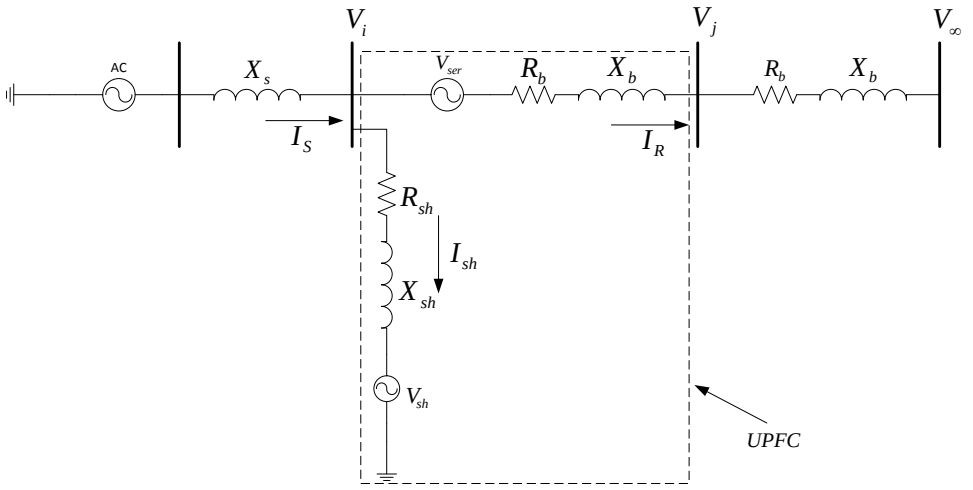

Figure 4.1: Single line diagram of the network including UPFC

In equation (4.1), V_{sh_x} is the real component, i.e. x-component, of V_{sh}. V_{sh} itself is the magnitude of the shunt voltage injected to the bus where the shunt branch of UPFC is connected to. δ_i is the phase angle of the bus voltage where the UPFC shunt branch is connected to the network. In the calculations presented here, δ_i is considered to be the phase reference of the network. ϕ is the phase difference between reference angle (δ_i) and shunt injected voltage angle (δ_{sh}).

$$V_{sh_x} = V_{sh}cos(\delta_i - \phi) \Rightarrow$$
$$\Delta V_{sh_x} = cos(\delta_i - \phi)\Delta V_{sh} - V_{sh}sin(\delta_i - \phi)\Delta\delta_i + V_{sh}sin(\delta_i - \phi)\Delta\phi \quad (4.1)$$

The phasor diagram for the voltages is shown in figure (4.2).

V_{sh_y} is the imaginary component, i.e. y-component, of V_{sh}. V_{sh}, δ_i, and ϕ are already defined.

$$V_{sh_y} = V_{sh}sin(\delta_i - \phi) \Rightarrow$$
$$\Delta V_{sh_y} = sin(\delta_i - \phi)\Delta V_{sh} + V_{sh}cos(\delta_i - \phi)\Delta\delta_i - V_{sh}cos(\delta_i - \phi)\Delta\phi \quad (4.2)$$

The magnitude of the shunt injected voltge is controlled using a PI controller. The block diagram including the PI controller is shown in figure (4.3). $V_{i_{ref}}$ is the desired voltage of the bus that the shunt branch of the UPFC is connected to. V_i is the magnitude of the bus voltage with the UPFC shunt branch connected to it.

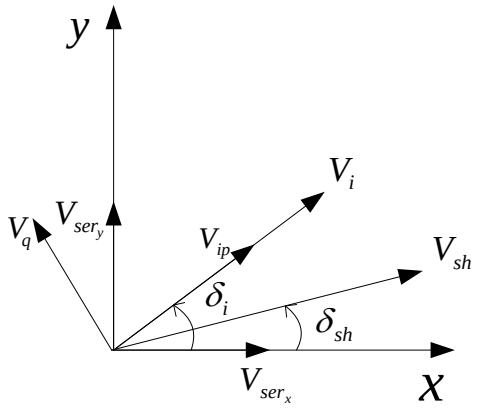

Figure 4.2: Phasor diagram for UPFC voltages

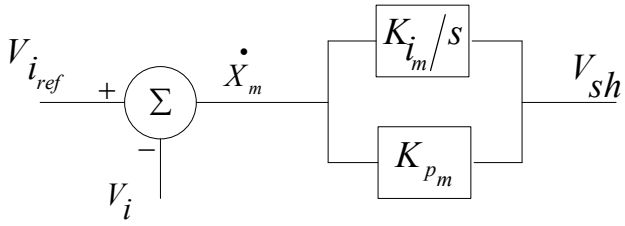

Figure 4.3: PI controller for the shunt injected voltage

$$V_{sh} = K_{i_m} X_m + \left(V_{i_{ref}} - V_i\right) K_{p_m} \Rightarrow$$
$$\Delta V_{sh} = K_{i_m} \Delta X_m + K_{p_m} \left(\Delta V_{i_{ref}} - \Delta V_i\right) \tag{4.3}$$

As mentioned previously, δ_i is the phase angle of the bus voltage where the UPFC shunt branch is connected to the rest of the network through that bus. If the x and y compenents of the bus voltage are known, the angle can be easily calculated using equation (4.4).

$$tan(\delta_i) = \frac{V_{i_y}}{V_{i_x}} \Rightarrow$$
$$sec^2 \delta_i \Delta\delta_i = -\frac{V_{i_y}}{V_{i_x}^2} \Delta V_{i_x} + \frac{1}{V_{i_x}} \Delta V_{i_y} \tag{4.4}$$

As explained earlier, V_i is the magnitude of the bus voltage with UPFC shunt branch connected to the bus. Equation (4.5) can be used to calculate V_i from V_{i_x} and V_{i_y}.

$$V_i = \sqrt{V_{i_x}^2 + V_{i_y}^2} \Rightarrow$$
$$V_i = \frac{V_{i_x}}{|V_i|}\Delta V_{i_x} + \frac{V_{i_y}}{|V_i|}\Delta V_{i_y} \tag{4.5}$$

ϕ is the output of the PI controller which controls the voltage across the DC capacitor in the UPFC. The corresponding PI controller is drawn in figure (4.4).

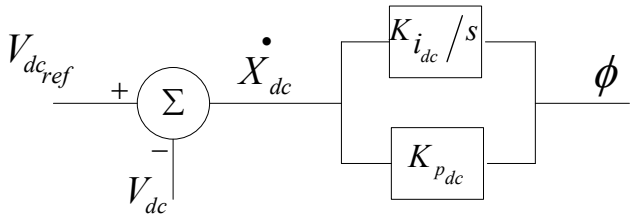

Figure 4.4: PI controller for DC voltage across the capacitor

$$\phi = K_{i_{dc}} X_{dc} + \left(V_{dc_{ref}} - V_{dc}\right) K_{p_{dc}} \Rightarrow$$
$$\Delta\phi = K_{i_{dc}} \Delta X_{dc} + K_{p_{dc}} \left(\Delta V_{dc_{ref}} - \Delta V_{dc}\right) \tag{4.6}$$

The series injected voltage to the line can be decomposed into two components in two different coordinates. One coordinate is the x-y coordinate. The other coordinate is in line with the reference angle, i.e. δ_i. One axis of this coordinate in in-phase with δ_i and the other axis is prependicular to it. V_{ser_x} is the x component of the series injected voltage to the line in the x-y coordinate. V_{ip} is the component of V_{ser} which is in-phase with δ_i. V_q is the component of V_{ser} which is quadrature to δ_i.

$$V_{ser_x} = V_{ip} cos(\delta_i) - V_q sin(\delta_i) \Rightarrow$$
$$\Delta V_{ser_x} = cos(\delta_i)\Delta V_{ip} - sin(\delta_i)\Delta V_q - \left(V_{ip} sin(\delta_i) + V_q cos(\delta_i)\right)\Delta\delta_i \tag{4.7}$$

V_{ser_y} is the y component of the series injected voltage to the line in the x-y coordinate.

$$V_{ser_y} = V_{ip} sin(\delta_i) + V_q cos(\delta_i) \Rightarrow$$
$$\Delta V_{ser_y} = sin(\delta_i)\Delta V_{ip} + cos(\delta_i)\Delta V_q + \left(V_{ip} cos(\delta_i) - V_q sin(\delta_i)\right)\Delta\delta_i \tag{4.8}$$

V_{ip} is the output of the PI controller that controls the reactive power flow in the line. The controller is shown in figure (4.5). Q_{ij} is the measured reactive power flow in the line.

Q_{ref} is the desired value of reactive power flow. $K_{i_{ip}}$ and $K_{p_{ip}}$ are integral and proportional gains of the controller respectively.

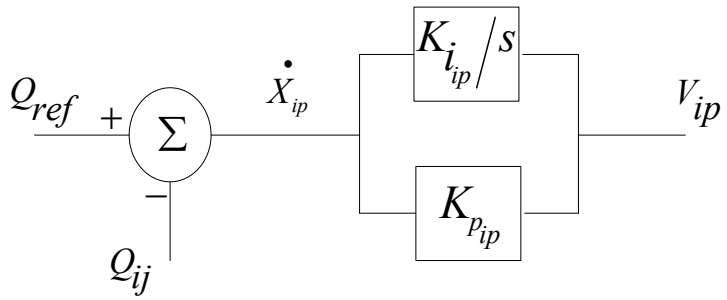

Figure 4.5: PI controller for the reactive power flow in the line

$$V_{ip} = K_{i_{ip}} X_{ip} + (Q_{ref} - Q_{ij})\, K_{p_{ip}} \Rightarrow$$
$$\Delta V_{ip} = K_{i_{ip}} \Delta X_{ip} + (\Delta Q_{ref} - \Delta Q_{ij})\, K_{p_{ip}} \tag{4.9}$$

V_q is the output of the PI controller that controls the active power flow in the line. The controller is shown in figure (4.6). P_{ij} is the measured active power flow in the line. P_{ref} is the desired value of active power flow. K_{i_q} and K_{p_q} are integral and proportional gains of the controller respectively.

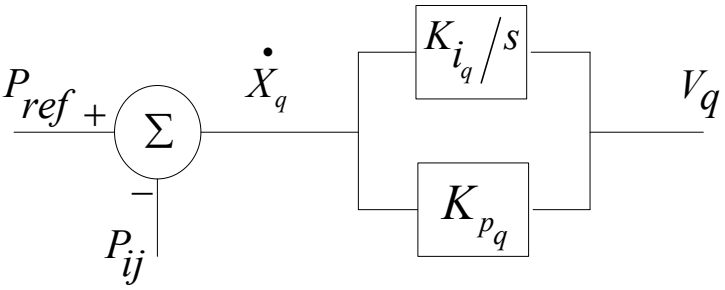

Figure 4.6: PI controller for the active power flow in the line

$$V_q = K_{i_q} X_q + (P_{ref} - P_{ij})\, K_{p_q} \Rightarrow$$
$$\Delta V_q = K_{i_q} \Delta X_q + (\Delta P_{ref} - \Delta P_{ij})\, K_{p_q} \tag{4.10}$$

P_{ij}, as explained before, is the active power flow in the line. V_{i_x} and V_{i_y} are x and y components of the sending bus voltage respectively. In the same way, V_{j_x} and V_{j_y} are x and

y components of the receiving bus voltage respectively. The coefficients P_1 to P_6 in this equation are given later in this chapter.

$$P_{ij} = Real(V_i^* I_{ij}) \Rightarrow$$
$$\Delta P_{ij} = P_1 \Delta V_{i_x} + P_2 \Delta V_{i_y} + P_3 \Delta V_{ser_x} + P_4 \Delta V_{ser_y} + P_5 \Delta V_{j_x} + P_6 \Delta V_{j_y} \quad (4.11)$$

Q_{ij}, as explained before, is the reactive power flow in the line. The coefficients Q_1 to Q_6 in this equation are given later in this chapter.

$$Q_{ij} = -Imag(V_i^* I_{ij}) \Rightarrow$$
$$\Delta Q_{ij} = Q_1 \Delta V_{i_x} + Q_2 \Delta V_{i_y} + Q_3 \Delta V_{ser_x} + Q_4 \Delta V_{ser_y} + Q_5 \Delta V_{j_x} + Q_6 \Delta V_{j_y} \quad (4.12)$$

After the steady state equations are defined, it is time to introduce the state and current injection equtions. Every dynamic device is defined with a set of state and current injection equations. The corresponding state and current equations for the UPFC power control mode is given in the following sets of formulas.

The UPFC P, Q control mode can be completely defined by five state variables. The derivative of the first state variable is defined as $\dot{X}_{dc}$ according to equation (4.13). It is the output of the summation block in figure (3.4).

$$\dot{X}_{dc} = \left(V_{dc_{ref}} - V_{dc}\right) \Rightarrow$$
$$\Delta \dot{X}_{dc} = \left(\Delta V_{dc_{ref}} - \Delta V_{dc}\right) \quad (4.13)$$

The second state variable that is used to define the UPFC model is X_m. The deravative of this state variable, i.e. $\dot{X}_m$ is the output of the summation block in figure (3.3).

$$\dot{X}_m = \left(V_{i_{ref}} - V_i\right) \Rightarrow$$
$$\Delta \dot{X}_m = \left(\Delta V_{i_{ref}} - \Delta V_i\right) \quad (4.14)$$

The third state variable is the DC voltage across the capacitor. Equation (4.15) is actually the power balance equation across the capacitor. Since all other equations are in p.u., this equation has also been converted to p.u. values. $Index_{dc}$ is the converting coefficient between actual and p.u. formula. To write the power balance equation across the capacitor in p.u., both sides of the equation need to be divided by base values for apparent power and DC voltage, i.e. S_b and V_{dc_b}. Then, $Index_{dc}$ can be calculated as $Index_{dc} = CV_{dc}^2/S_b$. P_{sh}

is the active power flow exchange between UPFC shunt branch and the sending bus in the network. P_{ser} is the active power flow exchange between the UPFC series branch and the network.

As it can be seen the first three state variable are common between the STATCOM and the UPFC. That is because the shunt branch of UPFC is actually a STATCOM.

$$\begin{aligned}
&\dot{V_{dc}} = \frac{(P_{sh} - P_{ser})}{Index_{dc} V_{dc}} \Rightarrow \\
&\Delta \dot{V_{dc}} = \frac{(\Delta P_{sh} - \Delta P_{ser})}{Index_{dc} V_{dc}} - \frac{(P_{sh} - P_{ser})\, \Delta V_{dc}}{Index_{dc} V_{dc}^2}
\end{aligned} \tag{4.15}$$

The forth state variable in the UPFC P, Q control mode, is X_q. The deravative of X_q is the output of the summation block in figure (4.6).

$$\begin{aligned}
&\dot{X_q} = (P_{ref} - P_{ii}) \Rightarrow \\
&\Delta \dot{X_q} = (\Delta P_{ref} - \Delta P_{ij})
\end{aligned} \tag{4.16}$$

Finally the last state variable is X_{ip}. As it can be seen in figure (4.5), its deravative is the difference between the measured and the desired value of reactive power flow. The last two state variables in the P, Q controller mode of the UPFC are associated with the series controllers.

$$\begin{aligned}
&\dot{X_{ip}} = (Q_{ref} - Q_{ij}) \Rightarrow \\
&\Delta \dot{X_{ip}} = (\Delta Q_{ref} - \Delta Q_{ij})
\end{aligned} \tag{4.17}$$

In addition to state space equations, the current injection formulas are also required to describe a dynamic device fully in small signal stability model. Equations (4.18)-(4.20) are those required for the UPFC model.

Equation (4.18) is the current that the shunt branch of the UPFC absorbs from the network. $(g_{sh} + jb_{sh})$ is the admittance of the exciter transformer that connects shunt branch of the UPFC to the network.

$$\begin{aligned}
I_{sh_x} + jI_{sh_y} &= \left(V_{i_x} + jV_{i_y} - V_{sh_x} - jV_{sh_y}\right)(g_{sh} + jb_{sh}) \Rightarrow \\
\Delta I_{sh_x} + j\Delta I_{sh_y} &= (g_{sh} + jb_{sh})\, \Delta V_{i_x} + (-b_{sh} + jg_{sh})\, \Delta V_{i_y} \\
&\quad - (g_{sh} + jb_{sh})\, \Delta V_{sh_x} + (b_{sh} - jg_{sh})\, \Delta V_{sh_y}
\end{aligned} \tag{4.18}$$

Equation (4.19) indicates the current that the UPFC is injecting to the network through the receiving bus of the UPFC. $(g_b + jb_b)$ is the admittance of the booster transformer that injects the voltage in series with the line to the network.

$$\begin{aligned}
&I_{R_x} + jI_{R_y} = \left(V_{i_x} + jV_{i_y} + V_{ser_x} + jV_{ser_y} - V_{j_x} - jV_{j_y}\right)(g_b + jb_b) \Rightarrow \\
&\Delta I_{R_x} + j\Delta I_{R_y} = (g_b + jb_b)\,\Delta V_{i_x} + (-b_b + jg_b)\,\Delta V_{i_y} \\
&\qquad\qquad + (g_b + jb_b)\,\Delta V_{ser_x} + (-b_b + jg_b)\,\Delta V_{ser_y} \\
&\qquad\qquad - (g_b + jb_b)\,\Delta V_{j_x} + (b_b - jg_b)\,\Delta V_{j_y}
\end{aligned} \tag{4.19}$$

The current I_S given in equation (4.20) is the current that the network is injecting to the sending end bus. It is actually the summation of I_{sh} and I_R. The formulas for the currents are written so that the direction of the currents are the same as what is shown in figure (4.1).

$$\begin{aligned}
&I_{S_x} + jI_{S_y} = I_{R_x} + jI_{R_y} + I_{sh_x} + jI_{sh_y} \Rightarrow \\
&\Delta I_{S_x} + j\Delta I_{S_y} = \left[(g_b + g_{sh}) + j\,(b_b + b_{sh})\right]\Delta V_{i_x} + \left[-\,(b_b + b_{sh}) + j\,(g_b + g_{sh})\right]\Delta V_{i_y} \\
&\qquad\qquad + (g_b + jb_b)\,\Delta V_{ser_x} + (-b_b + jg_b)\,\Delta V_{ser_y} \\
&\qquad\qquad - (g_b + jb_b)\,\Delta V_{j_x} + (b_b - jg_b)\,\Delta V_{j_y} \\
&\qquad\qquad + (-g_{sh} + jb_{sh})\,\Delta V_{sh_x} + (b_{sh} + jg_{sh})\,\Delta V_{sh_y}
\end{aligned} \tag{4.20}$$

If the linearized steady state equations, i.e. equation (4.1) to (4.12) are put together in a matrix format, the result is equation (4.21). In this equation, ΔZ is a set of intermediate variables; ΔX is the set of state equations; ΔU defines the inputs to the model and ΔV includes voltage of the buses with UPFC connected to them. Every single matrix in the following formulas is defined later in this section. As given in equation (4.25), UPFC can be ultimately written in state space model as a function of ΔX, ΔU and ΔV.

$$T\Delta Z + U\Delta X + V\Delta U + W\Delta V = 0 \tag{4.21}$$

In the same way, if the linearized state equations, equations (4.13)-(4.17), are combined together in a matrix format, it results in equation (4.22).

$$\Delta\,\dot{X} = M\Delta X + N\Delta U + O\Delta V + L\Delta Z \tag{4.22}$$

Equation (4.23) shows the linearized current interface between UPFC and the network. It combines the currents at the sending and receiving end into one single marix. The resultant equation (4.23), is the current injection equation for the UPFC when it is written in the

matrix form. It should be mentioned that the steady state, state space and current injection equations are organized to be written as a function of ΔX, ΔU, ΔV, and ΔZ.

$$\Delta I_{UPFC} = S_1 \Delta Z + S_2 \Delta V \tag{4.23}$$

As explained earlier, the goal is to describe the UPFC model in the standard state space format. To do so, ΔZ can be calculated as a function of ΔX, ΔU and ΔV from equation (4.21). Then, ΔZ is replaced in (4.22) and (4.23) to write $\Delta \dot{X}$ and ΔI_{UPFC} as a function of ΔX, ΔU and ΔV only, resulting in the final state and current equations for the dynamic device (see equation (4.25)).

$$\Delta Z = -T^{-1}U\Delta X - T^{-1}V\Delta U - T^{-1}W\Delta V \tag{4.24}$$

$$\begin{aligned} \Delta \dot{X}_d &= A_d \Delta X_d + B_d \Delta U_d + E_d \Delta V \\ \Delta I_d &= C_d \Delta X_d + D_d \Delta U_d + Y_d \Delta V \end{aligned} \tag{4.25}$$

$$A_d = \left(M - LT^{-1}U\right) \qquad B_d = \left(N - LT^{-1}V\right) \qquad E_d = \left(O - LT^{-1}W\right)$$

$$C_d = \left(-S_1T^{-1}U\right) \qquad D_d = \left(-S_1T^{-1}V\right) \qquad Y_d = \left(S_2 - S_1T^{-1}W\right)$$

Now that the UPFC state space model is derived, it has to be combined with the remaining part of the network. This is done through the current injection formula. In steady state, an AC network can be presented with its Y_{bus} matrix. Therefore, the current injection from the network side can be written as $\Delta I_{network} = Y_{bus}\Delta V$. On the other hand, based on the figure (4.1) and the way the UPFC current injection is formulated in equation (4.25), at the buses where the UPFC is connected to the network, the current from the network is equal and in the opposite direction of the current injection from UPFC. As a result, $\Delta I_{network} = -\Delta I_d$. By equating $\Delta I_{network}$ and ΔI_d, ΔV can be solved as in equation (4.26). Now if ΔV is replaced in (4.25), the system including the UPFC can be shown in standard state space format (equation (4.27)).

$$\Delta V = -(Y_N + Y_d)^{-1} C_d \Delta X - (Y_N + Y_d)^{-1} D_d \Delta U \tag{4.26}$$

$$\dot{X}_{sys} = A_{sys}\Delta X_{sys} + B_{sys}\Delta U \tag{4.27}$$

$$A_{sys} = A_d - E_d(Y_N + Y_d)^{-1}C_d \qquad B_{sys} = B_d - E_d(Y_N + Y_d)^{-1}D_d$$

$$M = \begin{bmatrix} 0 & 0 & -1 & 0 & 0 \\ 0 & 0 & 0 & 0 & 0 \\ 0 & 0 & -\frac{P_{sh}-P_{ser}}{Index_{dc}V_{dc}^2} & 0 & 0 \\ 0 & 0 & 0 & 0 & 0 \\ 0 & 0 & 0 & 0 & 0 \end{bmatrix} \quad O = \begin{bmatrix} 0 & 0 & 0 & 0 \\ 0 & 0 & 0 & 0 \\ \frac{\left(K_3-P_{ser_1}\right)}{Index_{dc}V_{dc}} & \frac{\left(K_4-P_{ser_2}\right)}{Index_{dc}V_{dc}} & \frac{-P_{ser_5}}{Index_{dc}V_{dc}} & \frac{-P_{ser_6}}{Index_{dc}V_{dc}} \\ 0 & 0 & 0 & 0 \\ 0 & 0 & 0 & 0 \end{bmatrix}$$

$$\Delta Z = \begin{bmatrix} \Delta V_{sh_x} \\ \Delta V_{sh_y} \\ \Delta V_{sh} \\ \Delta\phi \\ \Delta\delta_i \\ \Delta\left|V_i\right| \\ \Delta V_{ser_x} \\ \Delta V_{ser_y} \\ \Delta V_{ip} \\ \Delta V_q \\ \Delta P_{ij} \\ \Delta Q_{ij} \end{bmatrix} \quad \Delta X = \begin{bmatrix} \Delta X_{dc} \\ \Delta X_m \\ \Delta V_{dc} \\ \Delta X_{ip} \\ \Delta X_q \end{bmatrix} \quad \Delta U = \begin{bmatrix} \Delta V_{dc_{ref}} \\ \Delta V_{i_{ref}} \\ \Delta Q_{ref} \\ \Delta P_{ref} \end{bmatrix} \quad \Delta V = \begin{bmatrix} \Delta V_{i_x} \\ \Delta V_{i_y} \\ \Delta V_{j_x} \\ \Delta V_{j_y} \end{bmatrix} \quad \Delta I_d = \begin{bmatrix} \Delta I_{S_x} \\ \Delta I_{S_y} \\ -\Delta I_{R_x} \\ -\Delta I_{R_y} \end{bmatrix}$$

$$S_1 = \begin{bmatrix} -g_{sh} & b_{sh} & 0 & 0 & 0 & 0 & g_b & -b_b \\ -b_{sh} & -g_{sh} & 0 & 0 & 0 & 0 & b_b & g_b \\ 0 & 0 & 0 & 0 & 0 & 0 & -g_b & b_b \\ 0 & 0 & 0 & 0 & 0 & 0 & -b_b & -g_b \end{bmatrix} \quad S_2 = \begin{bmatrix} g_b + g_{sh} & -(b_b + b_{sh}) & -g_b & b_b \\ b_b + b_{sh} & g_b + g_{sh} & -b_b & -g_b \\ -g_b & b_b & g_b & -b_b \\ -b_b & -g_b & b_b & g_b \end{bmatrix}$$

$$N = \begin{bmatrix} 1 & 0 & 0 & 0 \\ 0 & 1 & 0 & 0 \\ 0 & 0 & 0 & 0 \\ 0 & 0 & 1 & 0 \\ 0 & 0 & 0 & 1 \end{bmatrix}$$

$$L = \begin{bmatrix} 0 & 0 & 0 & 0 & 0 & 0 & 0 & 0 & 0 & 0 & 0 & 0 \\ 0 & 0 & 0 & 0 & 0 & -1 & 0 & 0 & 0 & 0 & 0 & 0 \\ \frac{K_1}{Index_{dc}V_{dc}} & \frac{K_2}{Index_{dc}V_{dc}} & 0 & 0 & 0 & 0 & \frac{-P_{ser_3}}{Index_{dc}V_{dc}} & \frac{-P_{ser_4}}{Index_{dc}V_{dc}} & 0 & 0 & 0 & 0 \\ 0 & 0 & 0 & 0 & 0 & 0 & 0 & 0 & 0 & 0 & 0 & -1 \\ 0 & 0 & 0 & 0 & 0 & 0 & 0 & 0 & 0 & 0 & -1 & 0 \end{bmatrix}$$

$$U = \begin{bmatrix} 0 & 0 & 0 & 0 & 0 \\ 0 & 0 & 0 & 0 & 0 \\ 0 & K_{i_m} & 0 & 0 & 0 \\ K_{i_{dc}} & 0 & -K_{p_{dc}} & 0 & 0 \\ 0 & 0 & 0 & 0 & 0 \\ 0 & 0 & 0 & 0 & 0 \\ 0 & 0 & 0 & 0 & 0 \\ 0 & 0 & 0 & 0 & 0 \\ 0 & 0 & 0 & K_{i_{ip}} & 0 \\ 0 & 0 & 0 & 0 & K_{i_q} \\ 0 & 0 & 0 & 0 & 0 \\ 0 & 0 & 0 & 0 & 0 \end{bmatrix} \qquad V = \begin{bmatrix} 0 & 0 & 0 & 0 \\ 0 & 0 & 0 & 0 \\ 0 & K_{p_m} & 0 & 0 \\ K_{p_{dc}} & 0 & 0 & 0 \\ 0 & 0 & 0 & 0 \\ 0 & 0 & 0 & 0 \\ 0 & 0 & 0 & 0 \\ 0 & 0 & 0 & 0 \\ 0 & 0 & K_{p_{ip}} & 0 \\ 0 & 0 & 0 & K_{p_q} \\ 0 & 0 & 0 & 0 \\ 0 & 0 & 0 & 0 \end{bmatrix}$$

$$W = \begin{bmatrix} 0 & 0 & 0 & 0 \\ 0 & 0 & 0 & 0 \\ 0 & 0 & 0 & 0 \\ 0 & 0 & 0 & 0 \\ \frac{-V_{i_y}}{V_{i_x}^2} & \frac{1}{V_{i_x}} & 0 & 0 \\ \frac{V_{i_x}}{|V_i|} & \frac{V_{i_y}}{|V_i|} & 0 & 0 \\ 0 & 0 & 0 & 0 \\ 0 & 0 & 0 & 0 \\ 0 & 0 & 0 & 0 \\ 0 & 0 & 0 & 0 \\ P_1 & P_2 & P_5 & P_6 \\ Q_1 & Q_2 & Q_5 & Q_6 \end{bmatrix}$$

$$
T = \begin{bmatrix}
-1 & 0 & cos(\delta_i - \phi) & V_{sh}sin(\delta_i - \phi) & -V_{sh}sin(\delta_i - \phi) & 0 & 0 & 0 & 0 & 0 & 0 & 0 \\
0 & -1 & sin(\delta_i - \phi) & -V_{sh}cos(\delta_i - \phi) & V_{sh}cos(\delta_i - \phi) & 0 & 0 & 0 & 0 & 0 & 0 & 0 \\
0 & 0 & -1 & 0 & 0 & -K_{pm} & 0 & 0 & 0 & 0 & 0 & 0 \\
0 & 0 & 0 & -1 & 0 & 0 & 0 & 0 & 0 & 0 & 0 & 0 \\
0 & 0 & 0 & 0 & -sec^2(\delta_i) & 0 & 0 & 0 & 0 & 0 & 0 & 0 \\
0 & 0 & 0 & 0 & 0 & -1 & 0 & 0 & 0 & 0 & 0 & 0 \\
0 & 0 & 0 & 0 & -(V_{ip}sin(\delta_i) + V_q cos(\delta_i)) & 0 & -1 & 0 & cos(\delta_i) & -sin(\delta_i) & 0 & 0 \\
0 & 0 & 0 & 0 & (V_{ip}cos(\delta_i) - V_q sin(\delta_i)) & 0 & 0 & -1 & sin(\delta_i) & cos(\delta_i) & 0 & 0 \\
0 & 0 & 0 & 0 & 0 & 0 & 0 & 0 & -1 & 0 & 0 & -K_{p_{ip}} \\
0 & 0 & 0 & 0 & 0 & 0 & 0 & 0 & 0 & -1 & -K_{p_q} & 0 \\
0 & 0 & 0 & 0 & 0 & 0 & P_3 & P_4 & 0 & 0 & -1 & 0 \\
0 & 0 & 0 & 0 & 0 & 0 & Q_3 & Q_4 & 0 & 0 & 0 & -1
\end{bmatrix}
$$

P_1 to P_6 and Q_1 to Q_6 are the coefficients which have been used in linearized equations for active power flow, P_{ij}, (equation(4.11)) and reactive power flow, Q_{ij}, (equation (4.12)). Besides, the linearized equations for the active power flow in the shunt brunch, i.e P_{sh}, (equation (4.28)) as well as series injected active power flow, i.e P_{ser}, (equation (4.29)) and their corresponding coefficients are calculated in detail and are presented next.

$$P_1 = g_b V_{j_x} + b_b V_{j_y}$$

$$P_2 = -b_b V_{j_x} + g_b V_{j_y}$$

$$P_3 = g_b V_{j_x} + b_b V_{j_y}$$

$$P_4 = -b_b V_{j_x} + g_b V_{j_y}$$

$$P_5 = g_b \left(V_{i_x} + V_{ser_x} - V_{j_x}\right) - g_b V_{j_x} - b_b V_{j_y} - b_b \left(V_{i_y} + V_{ser_y} - V_{j_y}\right)$$

$$P_6 = b_b \left(V_{i_x} + V_{ser_x} - V_{j_x}\right) + b_b V_{j_x} - g_b V_{j_y} + g_b \left(V_{i_y} + V_{ser_y} - V_{j_y}\right)$$

$$Q_1 = b_b V_{j_x} - g_b V_{j_y}$$

$$Q_2 = g_b V_{j_x} + b_b V_{j_y}$$

$$Q_3 = b_b V_{j_x} - g_b V_{j_y}$$

$$Q_4 = g_b V_{j_x} + b_b V_{j_y}$$

$$Q_5 = g_b \left(V_{i_y} + V_{ser_y} - V_{j_y}\right) - b_b V_{j_x} + g_b V_{j_y} + b_b \left(V_{i_x} + V_{ser_x} - V_{j_x}\right)$$

$$Q_6 = b_b \left(V_{i_y} + V_{ser_y} - V_{j_y}\right) - g_b V_{j_x} - b_b V_{j_y} - g_b \left(V_{i_x} + V_{ser_x} - V_{j_x}\right)$$

$$P_{sh} = Real\left(V_{sh}^{*} I_{sh}\right) \tag{4.28}$$

$$P_{sh} = Real\left(\left(V_{sh_x} - jV_{sh_y}\right)\left(V_{i_x} + jV_{i_y} - V_{sh_x} - jV_{sh_y}\right)\left(g_{sh} + jb_{sh}\right)\right)$$

$$\Delta P_{sh} = P_{sh_1}\Delta V_{sh_x} + P_{sh_2}\Delta V_{sh_y} + P_{sh_3}\Delta V_{i_x} + P_{sh_4}\Delta V_{i_y}$$

$$P_{sh_1} = g_{sh}V_{i_x} - b_{sh}V_{i_y} - g_{sh}V_{sh_x} + b_{sh}V_{sh_y} - g_{sh}V_{sh_x} - b_{sh}V_{sh_y}$$

$$P_{sh_2} = b_{sh}V_{i_x} + g_{sh}V_{i_y} - b_{sh}V_{sh_x} - g_{sh}V_{sh_y} + b_{sh}V_{sh_x} - g_{sh}V_{sh_y}$$

$$P_{sh_3} = g_{sh}V_{sh_x} + b_{sh}V_{sh_y}$$

$$P_{sh_4} = -b_{sh}V_{sh_x} + g_{sh}V_{sh_y}$$

$$P_{ser} = Real\left(V_{ser}^{*}I_{ser}\right) \tag{4.29}$$

$$P_{ser} = Real\left(\left(V_{ser_x} - jV_{ser_y}\right)\left(V_{i_x} + jV_{i_y} + V_{ser_x} + jV_{ser_y} - V_{j_x} - jV_{j_y}\right)\left(g_b + jb_b\right)\right)$$

$$\Delta P_{ser} = P_{ser_1}\Delta V_{i_x} + P_{ser_2}\Delta V_{i_y} + P_{ser_3}\Delta V_{ser_x} + P_{ser_4}\Delta V_{ser_y} + P_{ser_5}\Delta V_{j_x} + P_{ser_6}\Delta V_{j_y}$$

$$P_{ser_1} = g_b V_{ser_x} + b_b V_{ser_y}$$

$$P_{ser_2} = -b_b V_{ser_x} + g_b V_{ser_y}$$

$$P_{ser_3} = g_b V_{i_x} + 2g_b V_{ser_x} - g_b V_{j_x} - b_b V_{i_y} + b_b V_{j_y}$$

$$P_{ser_4} = b_b V_{i_x} + 2g_b V_{ser_y} - b_b V_{j_x} - g_b V_{j_y} + g_b V_{i_y}$$

$$P_{ser_5} = -g_b V_{ser_x} - b_b V_{ser_y}$$

$$P_{ser_6} = b_b V_{ser_x} - g_b V_{ser_y}$$

4.1.1 Validation of the UPFC power control mode against PSCAD

In the previous section of this chapter, the SSS model for the UPFC power control mode was derived. The next step now, is to figure out whether the obtained model works as it is

expected or not. To do so, the SSS model is compared against the model which is bulit in PSCAD. It is worth mentioning that the UPFC shunt branch operates in the same manner as STATCOM. In other words, it controls the voltage at the sending end of the UPFC. Besides that, it absorbs/injects the active power flow from the network through the sending bus and transfers it to the series branch. The capacitor serves as a temporary energy storage. The voltage and hence the energy stored in the capacitor is held constant at steady state. Consequently, the net active power exchange between the UPFC and the network is zero in steady state condition.

As explained earlier in this chapter, UPFC power control model has four PI controllers. Two of them control the active and reactive power flow in the line, while the other two are responsible for maintaining the sending bus and capacitor voltage. In order to validate UPFC SSS model, a change has been made to the reference values of these controllers one at a time. The resultant waveforms from SSS model and PSCAD are then compared with each other. The results are shown individually in the remainder of this section.

- comparison of UPFC small signal model with PSCAD for changing the reference value of active power flow in the line

This part of section (4.1.1) shows the comparison between the PSCAD and SSS model when the reference MW value of active power flow in the line has been increased by 5 %. Figure (4.7) displays the active power flow in the line as the output. As per this comparison, the SSS model gives almost the same response as the PSCAD model for a change in the reference value of P. The next graph in figure (4.8) is considering the reactive power flow in the line as the system output. Based on the figure (4.8), the SSS model gives quite close response to PSCAD for the incremental change in P_{ref}.

Figure (4.9) shows the variation in the sending end bus voltage when the reference for the active power flow in the line has changed. Since this voltage is being controlled with a separate controller, a small change is expected in it which can be seen in the results from SSS and PSCAD model. Finally, the last comparison of this section is the DC voltage

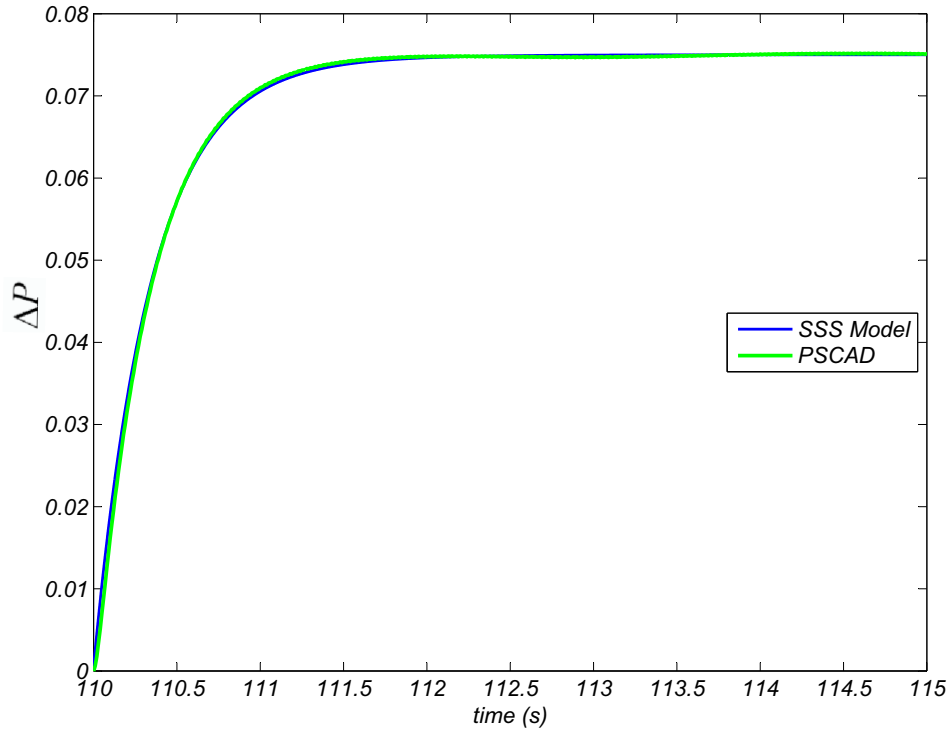

Figure 4.7: ΔP_{line} for a change in the reference value of P

across the capacitor (figure (4.10)). According to this figure, the SSS and PSCAD model are not giving the same results. The reason for this mismatch is not known and has been considered as future work to be done.

- comparison of UPFC small signal model with PSCAD for changing the reference value of reactive power flow in the line

In this section the SSS model will be compared versus PSCAD for a change in the reference value of reactive power flow in the line (Q_{ref}). For the first comparison, reactive power flow in the line has been drawn for both models in figure (4.11). From this figure, the SSS model and PSCAD are matching with each other. Figure (4.12) shows the active power flow in the line as the system output. Based on this figure the PSCAD curve is oscillating around the SSS model curve. This kind of oscillation is not unexpected for the PSCAD curve because PSCAD is taking the dynamics of the system into account while the SSS model does not.

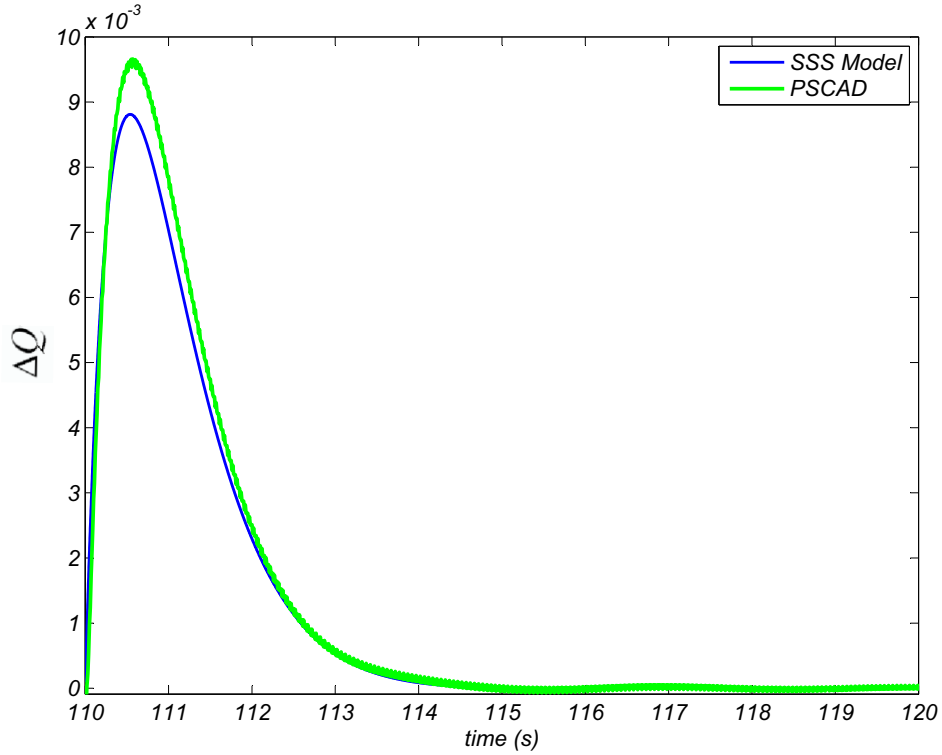

Figure 4.8: ΔQ_{line} for a change in the reference value of P

The next two figures give the sending end bus voltage and the DC bus voltage as the output respectively. Figure (4.13) shows a very small change in both models for the sending end voltage as a result of changing Q_{ref}. The amount of variation is expected based on the explanations given in the previous part of the results, for the same output but for a change in P_{ref}. Figure (4.14) compares the DC voltage in the two models. It is obvious from the figure that the models are completely different from DC voltage point of view.

- comparison of UPFC small signal model with PSCAD for changing the reference value of sending end bus voltage

For the last portion of validation of SSS model, the same four output as the last two comparisons are compared for a change in the reference value of the sending end bus voltage, $V_{i_{ref}}$. Figure (4.15) shows a good match between the two models for sending bus voltage. The curves drawn in figure (4.16) show the reactive power flow in the line for both models. It can be seen that the two graphs are very close to each other.

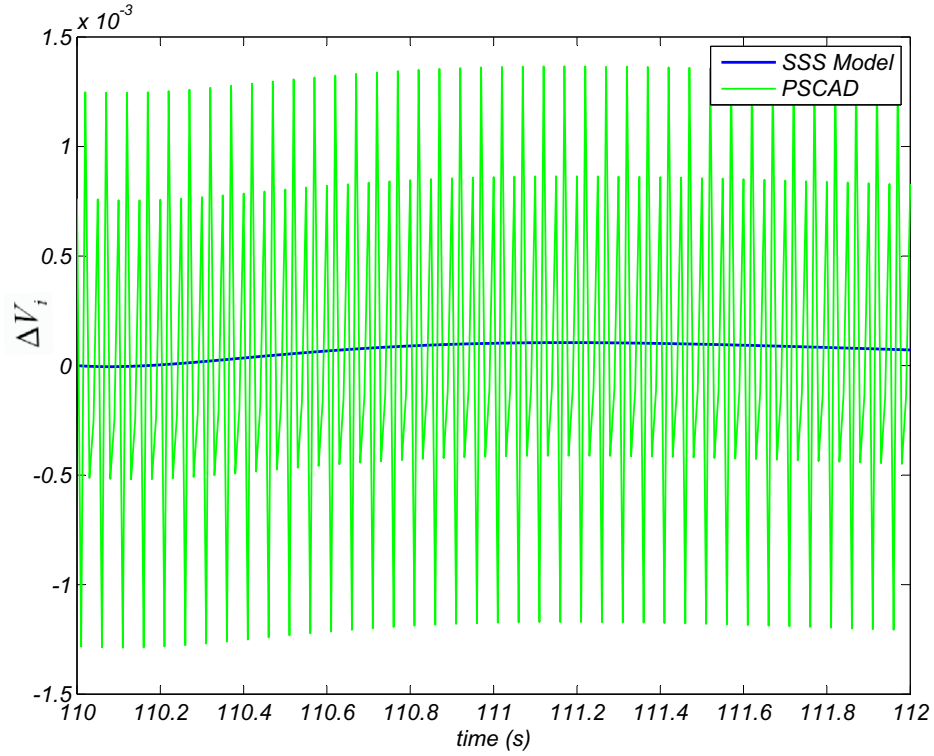

Figure 4.9: ΔV_i for a change in the reference value of P

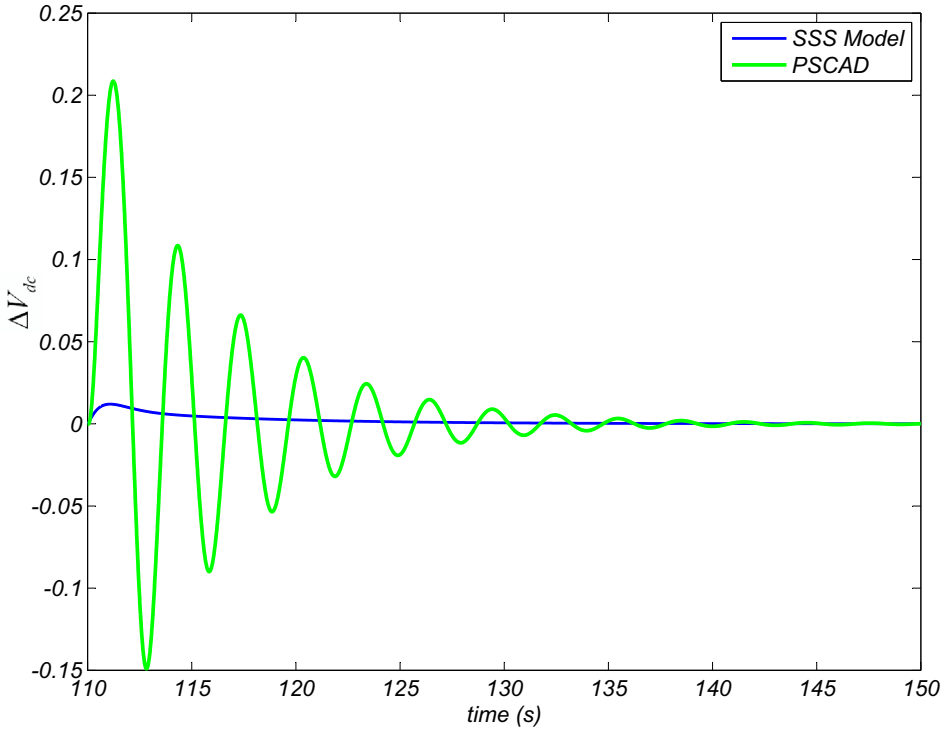

Figure 4.10: ΔV_{dc} for a change in the reference value of P

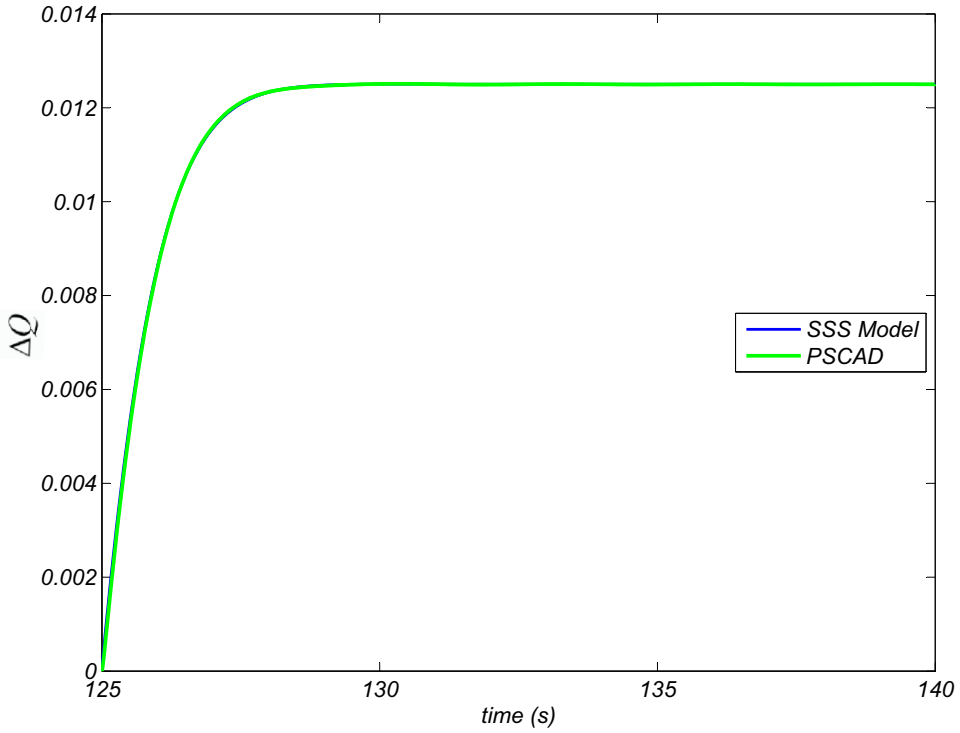

Figure 4.11: ΔQ_{line} for a change in the reference value of Q

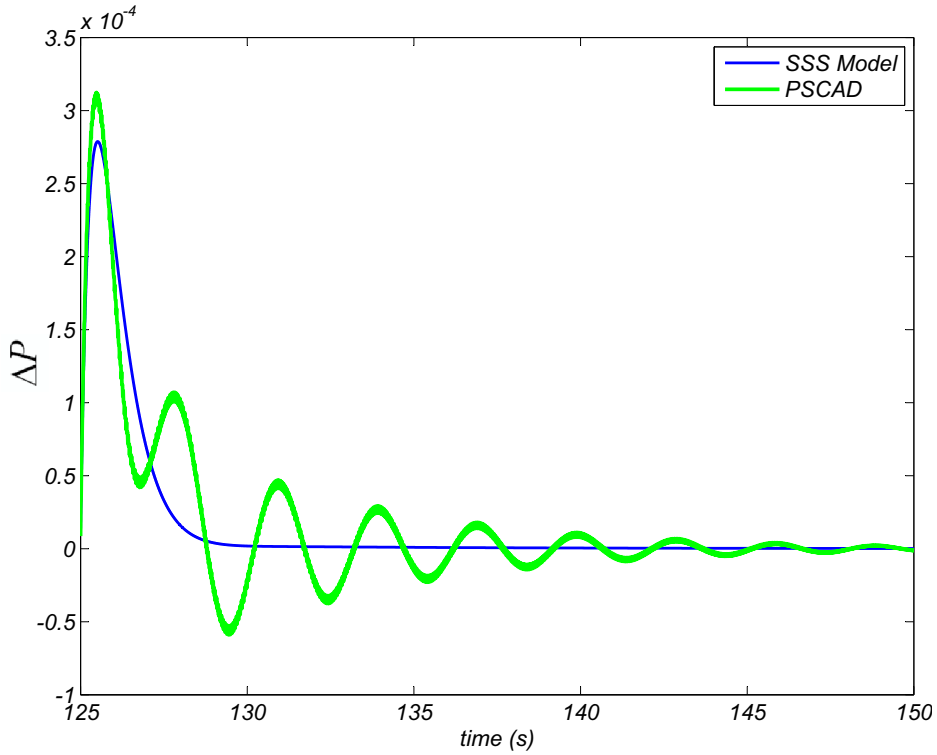

Figure 4.12: ΔP_{line} for a change in the reference value of Q

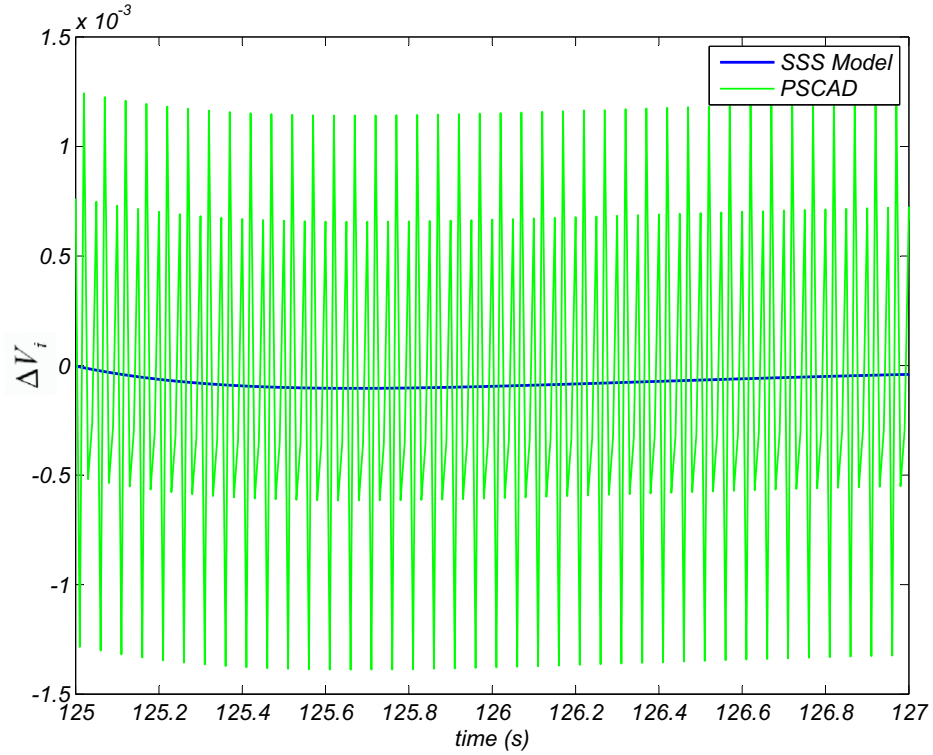

Figure 4.13: ΔV_i for a change in the reference value of Q

Lastly, the curves for active power flow in the line and the DC bus voltage are shown in figures (4.17) and (4.18). It is clear from the two figures that SSS model and PSCAD are different from each other. The reason for this difference needs more detailed investigations to be done as future work.

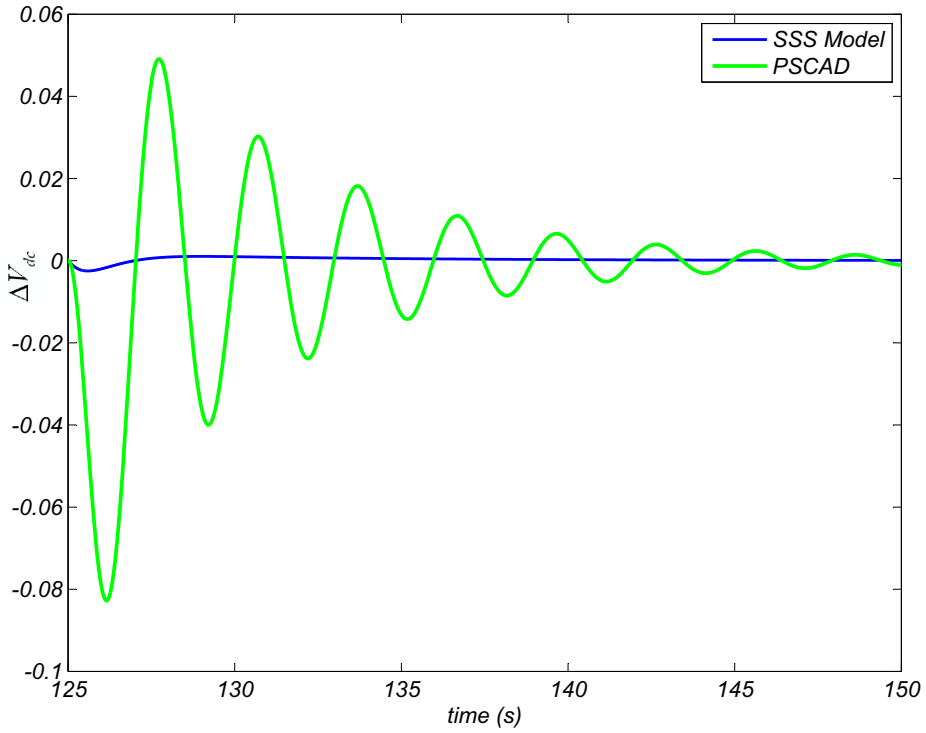

Figure 4.14: ΔV_{dc} for a change in the reference value of Q

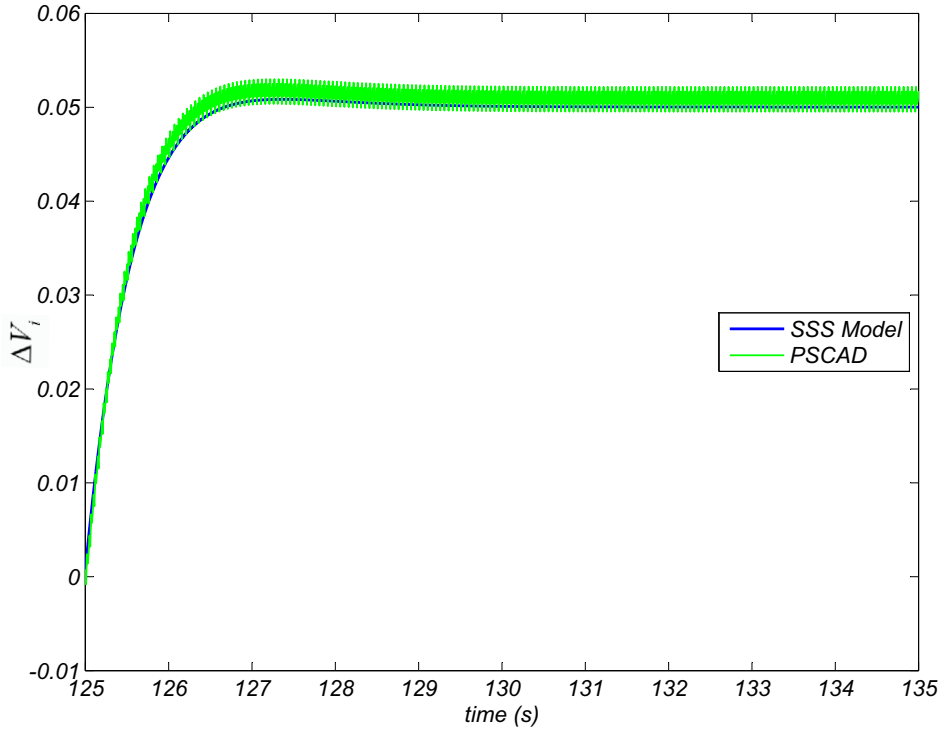

Figure 4.15: ΔV_i for a change in the reference value of V_i

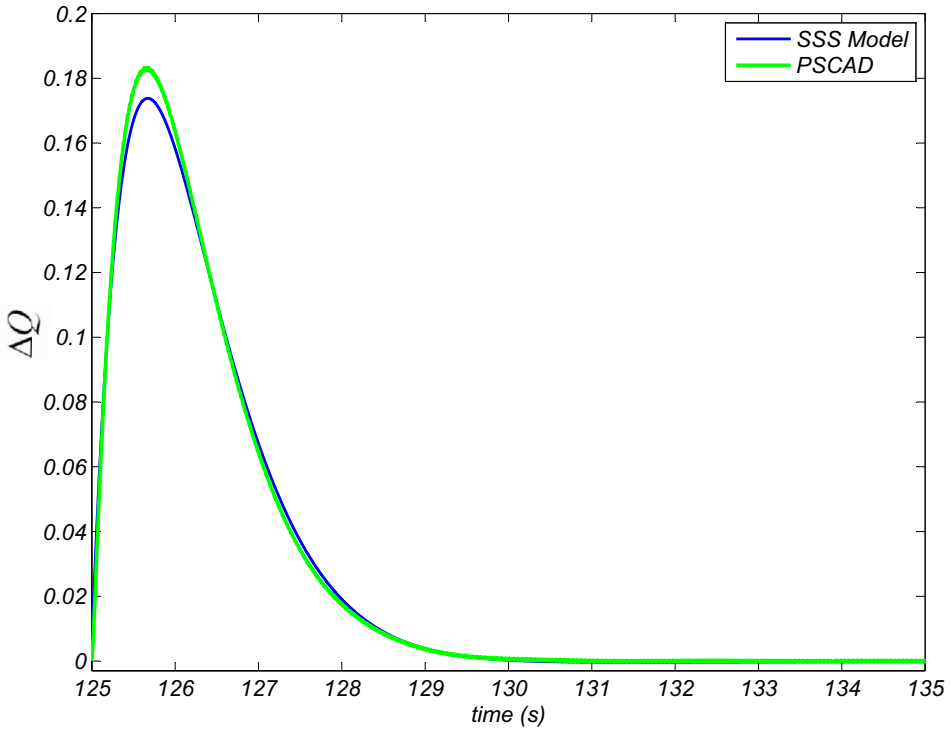

Figure 4.16: ΔQ_{line} for a change in the reference value of V_i

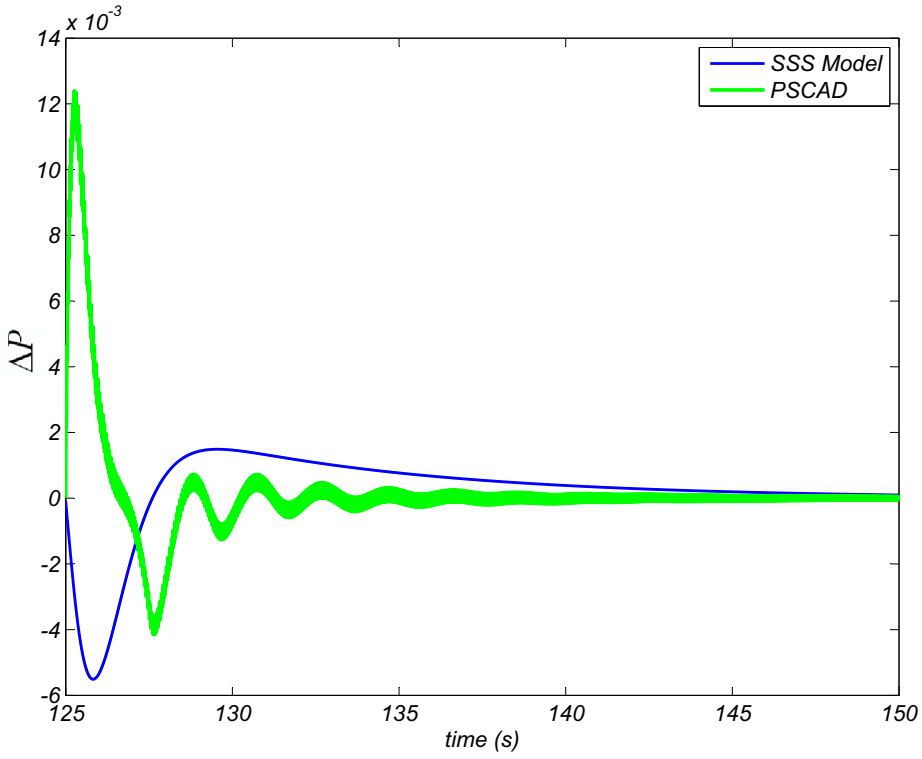

Figure 4.17: ΔP_{line} for a change in the reference value of V_i

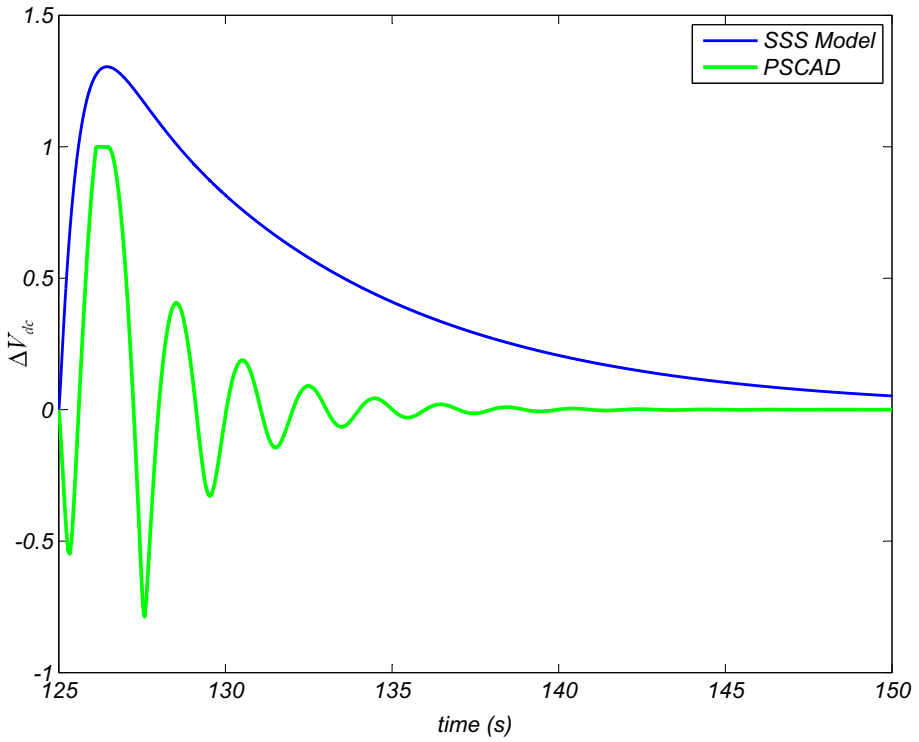

Figure 4.18: ΔV_{dc} for a change in the reference value of V_i

4.2 UPFC Voltage Control Mode Small Signal Model

This thesis introduced two control modes for the UPFC. The two models are exactly the same in the shunt brunch. Their difference is in the way the series brunch is modeled. The first model is the P, Q control mode. This mode of control, controls the active and reactive power flow in the line where the UPFC is connected to the network. The two series controllers in this model compare the measured active and reactive power flow in the line with their reference values. Then, based on the calculated difference, they inject voltage in series with the line to keep the power flow constant at the reference values. The other mode of control is the voltage control mode for UPFC. In this model, there is no feedback from the power flow in the line. Two voltage components are injected in series with the line. One of the components is in-phase with the sending end bus voltage; the other one is quadrature to the same voltage. The in-phase component changes the reactive power flow in the line and the quadrature one changes the active power flow.

The UPFC small signal model for power control mode was derived in section (4.1). This section is dedicated to small signal stability model for voltage control mode of UPFC. The procedure taken to develop the SSS model for voltage control mode is exactly the same as power control mode. It started with writing the steady state equations and followed by state space and current injection equations. Then the linearized equations have been put together in a matrix format. The resulted matrix equations have been simplified and combined to produce the final standard state space equation, i.e. $\dot{X} = A_{sys}\Delta X + B_{sys}\Delta U$. The exact details of the equations can be found in the remaining part of this section.

In equation (4.30), V_{sh_x} is the real component, i.e. x-component, of V_{sh}. V_{sh} itself is the magnitude of the shunt voltage injected to the bus where the shunt branch of the UPFC is connected to the network. δ_i is the phase angle of the bus voltage where the UPFC shunt branch is connected to. In the calculations presented here, δ_i is considered to be the phase reference of the network. ϕ is the phase difference between reference angle (δ_i) and shunt injected voltage angle (δ_{sh}).

$$V_{sh_x} = V_{sh}cos(\delta_i - \phi) \Rightarrow$$
$$\Delta V_{sh_x} = cos(\delta_i - \phi)\Delta V_{sh} - V_{sh}sin(\delta_i - \phi)\Delta\delta_i + V_{sh}sin(\delta_i - \phi)\Delta\phi \quad (4.30)$$

The phasor diagram for the voltages is shown in figure (4.19).

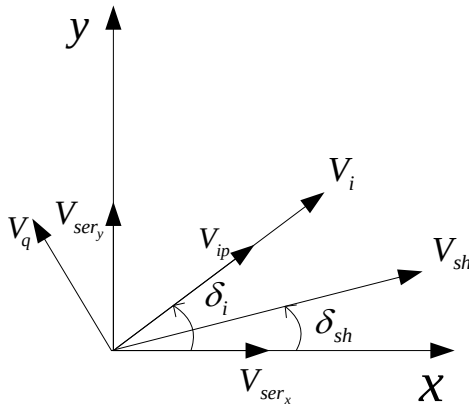

Figure 4.19: Phasor diagram for UPFC voltages

V_{sh_y} is the imaginary component, i.e. y-component, of V_{sh}. V_{sh}, δ_i, and ϕ are already defined.

$$V_{sh_y} = V_{sh} sin(\delta_i - \phi) \Rightarrow$$
$$\Delta V_{sh_y} = sin(\delta_i - \phi)\Delta V_{sh} + V_{sh} cos(\delta_i - \phi)\Delta\delta_i - V_{sh} cos(\delta_i - \phi)\Delta\phi \tag{4.31}$$

The magnitude of the shunt injected voltge is controlled using a PI controller. The block diagram including the PI controller is shown in figure (3.3). $V_{i_{ref}}$ is the desired voltage of the bus that the shunt branch of the UPFC is connected to. V_i is the magnitude of the bus voltage with the UPFC shunt branch connected to it.

$$V_{sh} = K_{i_m} X_m + \left(V_{i_{ref}} - V_i\right) K_{p_m} \Rightarrow$$
$$\Delta V_{sh} = K_{i_m} \Delta X_m + K_{p_m} \left(\Delta V_{i_{ref}} - \Delta V_i\right) \tag{4.32}$$

As explained earlier, δ_i is the phase angle of the bus voltage where the UPFC shunt branch is connected to the rest of the network through that bus. If the x and y compenents of the bus voltage are known, the angle can be easily calculated using equation (4.33).

$$tan(\delta_i) = \frac{V_{i_y}}{V_{i_x}} \Rightarrow$$
$$sec^2\delta_i \Delta\delta_i = -\frac{V_{i_y}}{V_{i_x}^2}\Delta V_{i_x} + \frac{1}{V_{i_x}}\Delta V_{i_y} \tag{4.33}$$

As mentioned previously, V_i is the magnitude of the bus voltage with UPFC shunt branch connected to the bus. Equation (4.34) can be used to calculate V_i from V_{i_x} and V_{i_y}.

$$V_i = \sqrt{V_{i_x}^2 + V_{i_y}^2} \Rightarrow$$
$$\Delta V_i = \frac{V_{i_x}}{|V_i|}\Delta V_{i_x} + \frac{V_{i_y}}{|V_i|}\Delta V_{i_y} \tag{4.34}$$

ϕ is the output of the PI controller which controls the voltage across the DC capacitor in UPFC. The corresponding PI controller is drawn in figure (3.4).

$$\phi = K_{i_{dc}} X_{dc} + \left(V_{dc_{ref}} - V_{dc}\right) K_{p_{dc}} \Rightarrow$$
$$\Delta\phi = K_{i_{dc}} \Delta X_{dc} + K_{p_{dc}} \left(\Delta V_{dc_{ref}} - \Delta V_{dc}\right) \tag{4.35}$$

The series injected voltage to the line can be decomposed into two components in two different coordinates. One coordinate is the x-y coordinate. The other coordinate is in line with the reference angle, i.e. δ_i. One axis of this coordinate is in-phase with δ_i and the other axis is prependicular to it. V_{ser_x} is the x component of the series injected voltage to

the line in the x-y coordinate. V_{ip} is the component of V_{ser} which is in-phase with δ_i. V_q is the component of V_{ser} which is quadrature to δ_i.

$$V_{ser_x} = V_{ip}cos(\delta_i) - V_q sin(\delta_i) \Rightarrow$$
$$\Delta V_{ser_x} = cos(\delta_i)\Delta V_{ip} - sin(\delta_i)\Delta V_q - (V_{ip}sin(\delta_i) + V_q cos(\delta_i))\,\Delta\delta_i \tag{4.36}$$

V_{ser_y} is the y component of the series injected voltage to the line in the x-y coordinate.

$$V_{ser_y} = V_{ip}sin(\delta_i) + V_q cos(\delta_i) \Rightarrow$$
$$\Delta V_{ser_y} = sin(\delta_i)\Delta V_{ip} + cos(\delta_i)\Delta V_q + (V_{ip}cos(\delta_i) - V_q sin(\delta_i))\,\Delta\delta_i \tag{4.37}$$

After the steady state equations are defined, it is time to introduce the state and current injection eqution. Every dynamic device is defined with a set of state and current injection equations. The corresponding state and current equations for the UPFC voltage control mode is given in the following sets of formulas.

The UPFC voltage control mode can be completely defined by three state variables, the same as the STATCOM. The derivative of the first state variable is determined as $\dot{X}_{dc}$ according to equation (4.38). It is the output of the summation block in the figure (3.4).

$$\dot{X}_{dc} = \left(V_{dc_{ref}} - V_{dc}\right) \Rightarrow$$
$$\Delta\,\dot{X}_{dc} = \left(\Delta V_{dc_{ref}} - \Delta V_{dc}\right) \tag{4.38}$$

The second state variable that is used to define the UPFC model is X_m. The deravative of this state variable, i.e. $\dot{X}_m$ is the output of the summation block in figure (3.3).

$$\dot{X}_m = \left(V_{i_{ref}} - V_i\right) \Rightarrow$$
$$\Delta\,\dot{X}_m = \left(\Delta V_{i_{ref}} - \Delta V_i\right) \tag{4.39}$$

The last state variable is the DC voltage across the capacitor. Equation (4.40) is actually the power balance equation across the capacitor. Since all other equations are in p.u., this equation has also been converted to p.u. values. $Index_{dc}$ is the converting coefficient between actual and p.u. formula. It is already defined in section (4.1). P_{sh} is the active power flow exchange between UPFC shunt brunch and the sending bus in the network. P_{ser} is the active power flow exchange between the UPFC series branch and the network.

As it can be seen, in the voltage control mode for UPFC, the state variables are the same

as the STATCOM. That is because the shunt branch of UPFC is actually a STATCOM and there is no series controller in this mode of control.

$$
\begin{aligned}
&CV_{dc}\,\dot{V}_{dc} = (P_{sh} - P_{ser}) \Rightarrow \\
&\Delta\,\dot{V}_{dc} = \frac{(\Delta P_{sh} - \Delta P_{ser})}{Index_{dc} V_{dc}} - \frac{(P_{sh} - P_{ser})\,\Delta V_{dc}}{Index_{dc} V_{dc}^2}
\end{aligned}
\tag{4.40}
$$

In addition to state space equations, the current injection formulas are also needed to describe a dynamic device fully in small signal stability model. Equations (4.41)-(4.43) are those required for the UPFC model.

Equation (4.41) is the current that the shunt branch of the UPFC absorbs from the network. $(g_{sh} + jb_{sh})$ is the admittance of the exciter transformer that connects shunt branch of the UPFC to the network.

$$
\begin{aligned}
&I_{sh_x} + jI_{sh_y} = \left(V_{i_x} + jV_{i_y} - V_{sh_x} - jV_{sh_y}\right)(g_{sh} + jb_{sh}) \Rightarrow \\
&\Delta I_{sh_x} + j\Delta I_{sh_y} = (g_{sh} + jb_{sh})\,\Delta V_{i_x} + (-b_{sh} + jg_{sh})\,\Delta V_{i_y} \\
&\qquad\qquad - (g_{sh} + jb_{sh})\,\Delta V_{sh_x} + (b_{sh} - jg_{sh})\,\Delta V_{sh_y}
\end{aligned}
\tag{4.41}
$$

Equation (4.42) indicates the current that the UPFC is injecting to the network through the receiving bus of the UPFC. $(g_b + jb_b)$ is the admittance of the booster transformer that injects the voltage in series with the line to the network.

$$
\begin{aligned}
&I_{R_x} + jI_{R_y} = \left(V_{i_x} + jV_{i_y} + V_{ser_x} + jV_{ser_y} - V_{j_x} - jV_{j_y}\right)(g_b + jb_b) \Rightarrow \\
&\Delta I_{R_x} + j\Delta I_{R_y} = (g_b + jb_b)\,\Delta V_{i_x} + (-b_b + jg_b)\,\Delta V_{i_y} \\
&\qquad\qquad + (g_b + jb_b)\,\Delta V_{ser_x} + (-b_b + jg_b)\,\Delta V_{ser_y} \\
&\qquad\qquad - (g_b + jb_b)\,\Delta V_{j_x} + (b_b - jg_b)\,\Delta V_{j_y}
\end{aligned}
\tag{4.42}
$$

The current I_S given in equation (4.43) is the current that the network is injecting to the sending end bus. It is actually the summation of I_{sh} and I_R. The formulas for the currents are written so that the direction of the currents are the same as what is shown in figure (4.1).

$$
\begin{aligned}
&I_{S_x} + jI_{S_y} = I_{R_x} + jI_{R_y} + I_{sh_x} + jI_{sh_y} \Rightarrow \\
&\Delta I_{S_x} + j\Delta I_{S_y} = [(g_b + g_{sh}) + j\,(b_b + b_{sh})]\,\Delta V_{i_x} + [-(b_b + b_{sh}) + j\,(g_b + g_{sh})]\,\Delta V_{i_y} \\
&\qquad\qquad + (g_b + jb_b)\,\Delta V_{ser_x} + (-b_b + jg_b)\,\Delta V_{ser_y} \\
&\qquad\qquad - (g_b + jb_b)\,\Delta V_{j_x} + (b_b - jg_b)\,\Delta V_{j_y} \\
&\qquad\qquad + (-g_{sh} + jb_{sh})\,\Delta V_{sh_x} + (b_{sh} + jg_{sh})\,\Delta V_{sh_y}
\end{aligned}
\tag{4.43}
$$

If the linearized steady state equations, i.e. equation (4.30) to (4.37) are put together in a matrix format, the result is equation (4.44). In this equation, ΔZ is a set of intermediate variables; ΔX is the set of state equations; ΔU defines the inputs to the model and ΔV includes voltage of the buses with UPFC connected to them. Each matrix in the following formulas is defined later in this section. As it is given in equation (4.48), the UPFC can be ultimately written, in state space model, as a function of ΔX, ΔU and ΔV.

$$T\Delta Z + U\Delta X + V\Delta U + W\Delta V = 0 \tag{4.44}$$

In the same way, if the linearized state equations, equations (4.38)-(4.40), are combined together in a matrix format, it results in equation (4.45).

$$\Delta \dot{X} = M\Delta X + N\Delta U + O\Delta V + L\Delta Z \tag{4.45}$$

Equation (4.46) shows the linearized current interface between UPFC and the network. It combines the currents at the sending and receiving end into one single marix. The resultant equation (4.46), is the current injection equation for the UPFC when it is written in the matrix form. It should be mentioned that the steady state, state space and current injection equations are organized to be written as a function of ΔX, ΔU, ΔV, and ΔZ.

$$\Delta I_{UPFC} = S_1\Delta Z + S_2\Delta V \tag{4.46}$$

As it was explained earlier, the goal is to describe the UPFC model in the standard state space format. To do so, ΔZ can be calculated as a function of ΔX, ΔU and ΔV from equation (4.44). Then, ΔZ is replaced in (4.45) and (4.46) to write $\Delta \dot{X}$ and ΔI_{UPFC} as a function of ΔX, ΔU and ΔV, resulting in the final state and current equations for the dynamic device (equation (4.48)).

$$\Delta Z = -T^{-1}U\Delta X - T^{-1}V\Delta U - T^{-1}W\Delta V \tag{4.47}$$

$$\begin{aligned} \Delta \dot{X}_d &= A_d\Delta X_d + B_d\Delta U_d + E_d\Delta V \\ \Delta I_d &= C_d\Delta X_d + D_d\Delta U_d + Y_d\Delta V \end{aligned} \tag{4.48}$$

Now that the UPFC state space model is derived, it has to be combined with the remaining part of the network. This is done through the current injection formula. In steady

state, an AC network can be presented with its Y_{bus} matrix. Therefore, the current injection from the network side can be written as $\Delta I_{network} = Y_{bus}\Delta V$. On the other hand, based on figure (4.1) and the way the UPFC current injection is formulated in equation (4.48), at the buses where the UPFC is connected to the network, the current from the network is equal and in the opposite direction of the current injection from the UPFC. As a result, $\Delta I_{network} = -\Delta I_d$. By equating $\Delta I_{network}$ and ΔI_d, ΔV can be solved as in equation (4.49). Now if ΔV is replaced in (4.48), the system including the UPFC can be shown in standard state space format (equation (4.50)).

$$\Delta V = -(Y_N + Y_d)^{-1} C_d \Delta X - (Y_N + Y_d)^{-1} D_d \Delta U \tag{4.49}$$

$$\dot{X}_{sys} = A_{sys}\Delta X_{sys} + B_{sys}\Delta U \tag{4.50}$$

$$A_{sys} = A_d - E_d(Y_N + Y_d)^{-1} C_d \qquad B_{sys} = B_d - E_d(Y_N + Y_d)^{-1} D_d$$

$$A_d = \left(M - LT^{-1}U\right) \qquad B_d = \left(N - LT^{-1}V\right) \qquad E_d = \left(O - LT^{-1}W\right)$$

$$C_d = \left(-S_1T^{-1}U\right) \qquad D_d = \left(-S_1T^{-1}V\right) \qquad Y_d = \left(S_2 - S_1T^{-1}W\right)$$

$$T = \begin{bmatrix} -1 & 0 & cos(\delta_i - \phi) & V_{sh}sin(\delta_i - \phi) & -V_{sh}sin(\delta_i - \phi) & 0 & 0 & 0 \\ 0 & -1 & sin(\delta_i - \phi) & -V_{sh}cos(\delta_i - \phi) & V_{sh}cos(\delta_i - \phi) & 0 & 0 & 0 \\ 0 & 0 & -1 & 0 & 0 & -K_{pm} & 0 & 0 \\ 0 & 0 & 0 & -1 & 0 & 0 & 0 & 0 \\ 0 & 0 & 0 & 0 & -sec^2(\delta_i) & 0 & 0 & 0 \\ 0 & 0 & 0 & 0 & 0 & -1 & 0 & 0 \\ 0 & 0 & 0 & 0 & -V_{ip}sin(\delta_i) - V_q cos(\delta_i) & 0 & -1 & 0 \\ 0 & 0 & 0 & 0 & V_{ip}cos(\delta_i) - V_q sin(\delta_i)) & 0 & 0 & -1 \end{bmatrix}$$

$$U = \begin{bmatrix} 0 & 0 & 0 \\ 0 & 0 & 0 \\ 0 & K_{i_m} & 0 \\ K_{i_{dc}} & 0 & -K_{p_{dc}} \\ 0 & 0 & 0 \\ 0 & 0 & 0 \\ 0 & 0 & 0 \\ 0 & 0 & 0 \end{bmatrix} \quad V = \begin{bmatrix} 0 & 0 & 0 & 0 \\ 0 & 0 & 0 & 0 \\ 0 & K_{p_m} & 0 & 0 \\ K_{p_{dc}} & 0 & 0 & 0 \\ 0 & 0 & 0 & 0 \\ 0 & 0 & 0 & 0 \\ 0 & 0 & cos(\delta_i) & -sin(\delta_i) \\ 0 & 0 & cs(\delta_i) & cos(\delta_i) \end{bmatrix} \quad W = \begin{bmatrix} 0 & 0 & 0 & 0 \\ 0 & 0 & 0 & 0 \\ 0 & 0 & 0 & 0 \\ 0 & 0 & 0 & 0 \\ \frac{-V_{iy}}{V_{ix}^2} & \frac{1}{V_{ix}} & 0 & 0 \\ \frac{V_{ix}}{\lvert V_i \rvert} & \frac{V_{iy}}{\lvert V_i \rvert} & 0 & 0 \end{bmatrix}$$

$$M = \begin{bmatrix} 0 & 0 & -1 \\ 0 & 0 & 0 \\ 0 & 0 & -\frac{(P_{sh} - P_{ser})}{Index_{dc}V_{dc}} \\ 0 & 0 & 0 \\ 0 & 0 & 0 \end{bmatrix} \quad O = \begin{bmatrix} 0 & 0 & 0 & 0 \\ 0 & 0 & 0 & 0 \\ \frac{(k_3 - P_{ser_1})}{Index_{dc}V_{dc}} & \frac{(k_4 - P_{ser_2})}{Index_{dc}V_{dc}} & \frac{-P_{ser_5}}{Index_{dc}V_{dc}} & \frac{-P_{ser_6}}{Index_{dc}V_{dc}} \end{bmatrix}$$

$$N = \begin{bmatrix} 1 & 0 & 0 & 0 \\ 0 & 1 & 0 & 0 \\ 0 & 0 & 0 & 0 \end{bmatrix} \quad L = \begin{bmatrix} 0 & 0 & 0 & 0 & 0 & 0 & 0 & 0 \\ 0 & 0 & 0 & 0 & 0 & -1 & 0 & 0 \\ \frac{k_1}{Index_{dc}V_{dc}} & \frac{k_2}{Index_{dc}V_{dc}} & 0 & 0 & 0 & 0 & \frac{-P_{ser_3}}{Index_{dc}V_{dc}} & \frac{-P_{ser_4}}{Index_{dc}V_{dc}} \end{bmatrix}$$

$$\Delta Z = \begin{bmatrix} \Delta V_{sh_x} \\ \Delta V_{sh_y} \\ \Delta V_{sh} \\ \Delta \phi \\ \Delta \delta_i \\ \Delta |V_i| \\ \Delta V_{ser_x} \\ \Delta V_{ser_y} \end{bmatrix} \quad \Delta X = \begin{bmatrix} \Delta X_{dc} \\ \Delta X_m \\ \Delta V_{dc} \end{bmatrix} \quad \Delta U = \begin{bmatrix} \Delta V_{dc_{ref}} \\ \Delta V_{i_{ref}} \\ \Delta V_{ip_{ref}} \\ \Delta V_{q_{ref}} \end{bmatrix} \quad \Delta V = \begin{bmatrix} \Delta V_{i_x} \\ \Delta V_{i_y} \\ \Delta V_{j_x} \\ \Delta V_{j_y} \end{bmatrix} \quad \Delta I_d = \begin{bmatrix} \Delta I_{S_x} \\ \Delta I_{S_y} \\ -\Delta I_{R_x} \\ -\Delta I_{R_y} \end{bmatrix}$$

$$S_1 = \begin{bmatrix} -g_{sh} & b_{sh} & 0 & 0 & 0 & 0 & g_b & -b_b \\ -b_{sh} & -g_{sh} & 0 & 0 & 0 & 0 & b_b & g_b \\ 0 & 0 & 0 & 0 & 0 & 0 & -g_b & b_b \\ 0 & 0 & 0 & 0 & 0 & 0 & -b_b & -g_b \end{bmatrix} \quad S_2 = \begin{bmatrix} g_b + g_{sh} & -(b_b + b_{sh}) & -g_b & b_b \\ b_b + b_{sh} & g_b + g_{sh} & -b_b & -g_b \\ -g_b & b_b & g_b & -b_b \\ -b_b & -g_b & b_b & g_b \end{bmatrix}$$

4.2.1 Validation of UPFC voltage control mode against nonlinear equations

The UPFC small signal stability model for the voltage control mode is validated in this section. The model has been validated against nonlinear equations. To do so, the network shown in figure (4.1) has been solved for two different steady state conditions. In each steady state condition, the system variables such as voltage magnitudes and angles, power flows, state variables and etc have been calculated. Then from these calculations, ΔZ, ΔX, ΔV, and ΔU have been determined. The calculated variations are then substituted

Table 4.1: Caclulated intermidiate variables and their variations for two steady states

intermediate variable	$V_{q_1} = 0.0809$	$V_{q_2} = 0.0849$
V_{sh_x}	1.2261	1.2207
V_{sh_y}	0.1688	0.2046
V_{sh}	1.2377	1.2377
ϕ	-0.0132	-0.0425
δ_i	0.1236	0.1236
V_i	1.02	1.02
V_{ser_x}	-0.0108	-0.0614
V_{ser_y}	0.0802	0.0587

Table 4.2: Caclulated UPFC end voltages and their variations for two steady states

voltage	$V_{q_1} = 0.0809$	$V_{q_2} = 0.0849$
V_{i_x}	1.0122	1.0122
V_{i_y}	0.1258	0.1258
V_{j_x}	1.0012	0.9616
V_{j_y}	0.1607	0.1439

into equation (4.44). It can be seen that the calculated variations from solving the nonlinear system, satisfy the linearized equations. As a result, it can be concluded that the linearized model is accurate.

- Validation of UPFC small signal model for voltage control mode for a step change in the value of the quadrature component of the series injected voltage

For the first set of results, the value of quadrature component of the series injected voltage, V_q, is increased by 5 %. The initial value of V_q is 0.0809 and the final value is 0.0849. The calculated system variables for both steady states are presented in tables (4.1) to (4.4).

Table 4.3: Caclulated system inputs and their variations for two steady states

input	$V_{q_1} = 0.0809$	$V_{q_2} = 0.0849$
$V_{dc_{ref}}$	1	1
$V_{i_{ref}}$	1.02	1.02
$V_{ip_{ref}}$	-0.00081	-0.00081
$V_{q_{ref}}$	0.0809	0.0849

Table 4.4: Caclulated state variables and their variations for two steady states

state variable	$V_{q_1} = 0.0809$	$V_{q_2} = 0.0849$
X_{dc}	-0.6596	-2.1236
X_m	0.0179	0.0179
V_{dc}	1	1

Table 4.5: Caclulated final result for validation of the model

result
5.569×10^{-4}
8.1875×10^{-5}
0
3.4694×10^{-18}
4.0613×10^{-18}
-3.4221×10^{-18}
0.0502
0.0255

Now if the difference between columns three and two in tables (4.1) to (4.4) are calculated and inserted into equation (4.44), the result of the calculation would be zero as is expected. The numerical values of the results are given in table (4.5).

- Validation of UPFC small signal model for voltage control mode for a step change in the value of the in-phase component of the series injected voltage

In this section, the value of the in-phase component of the series injected voltage, V_{ip}, is increased by 5 %. The initial value of V_{ip} is -0.00081 and the final value is -0.0008505. The calculated system variables for both steady states are presented in tables (4.6) to (4.9).

Now if the difference between columns three and two in tables (4.6) to (4.9) are calculated and substituted into equation (4.44), the result of the calculation would be zero as is expected. The numerical values of the results are given in table (4.10).

According to the final results given in tables (4.5) and (4.10), it can be understood that the small signal model introduced for UPFC voltage control mode matches with the nonlinear solutions. Therefore, it can be concluded that the SSS model is accurate and correct except for the last two equations that show 5 % and 2 % errors when the value of V_q is increased by 5 %. However, the errors can be considered small.

Table 4.6: Caclulated intermidiate variables and their variations for two steady states

intermediate variable	$V_{ip_1} = -0.00081$	$V_{ip_2} = -0.0008505$
V_{sh_x}	1.226287	1.226279
V_{sh_y}	0.16769	0.16775
V_{sh}	1.2377	1.2377
ϕ	-0.012298	-0.012345
δ_i	0.1236	0.1236
V_i	1.02	1.02
V_{ser_x}	-0.010778	-0.010818
V_{ser_y}	0.0801829	0.0801779

Table 4.7: Caclulated UPFC end voltages and their variations for two steady states

voltage	$V_{ip_1} = -0.00081$	$V_{ip_2} = -0.0008505$
V_{i_x}	1.0122	1.0122
V_{i_y}	0.1258	0.1258
V_{j_x}	1.001513	1.001473
V_{j_y}	0.161434	0.161427

Table 4.8: Caclulated system inputs and their variations for two steady states

input	$V_{ip_1} = -0.00081$	$V_{ip_2} = -0.0008505$
$V_{dc_{ref}}$	1	1
$V_{i_{ref}}$	1.02	1.02
$V_{ip_{ref}}$	-0.00081	-0.0008505
$V_{q_{ref}}$	0.0809	0.0809

Table 4.9: Caclulated state variables and their variations for two steady states

state variable	$V_{ip_1} = -0.00081$	$V_{ip_2} = -0.0008505$
X_{dc}	-0.6149	-0.6173
X_m	0.0179	0.0179
V_{dc}	1	1

Table 4.10: Caclulated final result for validation of the model

result
1.3681×10^{-9}
1.8710×10^{-10}
-1.7228×10^{-17}
-1.2875×10^{-19}
0
0
1.2875×10^{-19}
-4.5706×10^{-18}

5 Conclusions

A new small signal stability control mode for the UPFC was introduced in this thesis. In addition to that, a straightforward systematic procedure for deriving a small signal stability model of any dynamic device was demonstrated.

From different categories of FACTS devices, which have been summarized in chapter (1), this research has focused on STATCOM and UPFC.

Chapter (2) introduced two models that were proposed for UPFC. The behavior of the models was compared from transient stability point of view; and advantages and disadvantageous of each model were discussed. Based on the results shown, the transient behavior of the model depends on the location of the fault in the system. The short circuit capacity of the bus at which the fault occurs is also an important factor. In this case, it has been observed that both power control and voltage control modes are stable for a fault at the sending end of the UPFC where it is connected to a synchronous machine. However, for a fault at the end of the transmission line and close to the infinite bus, the voltage control mode stays stable while the power control mode becomes unstable if the outputs of the PI controllers are not limited. This demonstrate one case where P, Q control mode is not suitable. This observation indicates that the right mode of control should be chosen depending on the network and the location of the UPFC. This is one reason that it became our interest to develop the small signal stability model for both modes of control. It should be mentioned that some cases can also be found wherre P, Q control mode shows a better performance than voltage control mode.

Chapters (3) and (4) show how to derive the small signal stability model using the proposed systematic method for STATCOM and UPFC respectively. The proposed method is a simple procedure of developing a small signal stability model step by step. It can be used for any single dynamic device.

Once the small signal model was finalized, it was compared with the same model in PSCAD. The curves including the comparisons of the SSS model and PSCAD model were

shown in detail in chapter (3) for STATCOM. The results show a close match between the SSS and PSCAD model. Based on the results shown in chapter (3), the network variables show similar behavior in both models for changing reference values of controllers. The state variables used to describe the system in state space, and therefore in forming the small signal stability model, have been also compared for STATCOM. The compared results for state variables were also close in both models.

In chapter (4) the small signal model of the UPFC for both modes of control were validated. The power control mode of the UPFC was validated against PSCAD. The simulation results are matched appropriately with PSCAD for network variables. It was shown that the active and reactive power flow in the line, as well as the AC bus voltage were quite close to each other in small signal stability model and PSCAD when the reference values of voltage and active and reactive power flow are changing. However, a mismatch between the two models in DC voltage across the capacitor was also observed.

Since active power flow in the line and DC voltage across the capacitor are interconnected through the power balance equation across the DC link, it can be understood that aside from DC voltage, the active power flow from the small signal stability model was also not matching with PSCAD when the reference value of AC voltage was changing.

For UPFC voltage control mode, the small signal stability model was validated against nonlinear solution of the network. The results showed a good match between the small signal stability model and nonlinear equations. It can be observed from the final result tables for the voltage control mode in chapter (4), that the matrices describing the UPFC in small signal stability model satisfy the nonlinear solution of the network. The comparison was done for changing the value of in-phase and quadrature component of the injected voltage. In both situations, the small signal model matrices satisfied the results of solving nonlinear equations for the network. The difference between small signal stability model and nonlinear equations is acceptable.

To summarize, the results presented in chapter (2) emphasize the importance of modeling a new control mode for UPFC. The results shown in chapters (3) and (4) explain the

steps of developing the model and the procedure for validation of models. A systematic and easy approach was used to model the dynamic devices in state space. The proposed procedure is easy to follow and understand and can be used to model any dynamic device.

References

[1] S. Jiang, "Modelling and validation of small signal models of vsc-based facts devices embedded in large ac networks," Ph.D. dissertation, Department of Electrical and Computer Engineering, University of Manitoba, 2010.

[2] P. Kundur, N. Balu, and M. Lauby, *Power system stability and control*. McGraw-Hill New York, 1994.

[3] N. Hingorani and L. Gyugyi, *Understanding FACTS: concepts and technology of flexible AC transmission systems*. IEEE Press, 2000.

[4] N. Hingorani, "Facts-flexible ac transmission system," in *AC and DC Power Transmission, 1991., International Conference on*, 1991, pp. 1 –7.

[5] J. Chen, T. Lie, and D. Vilathgamuwa, "Enhancement of power system damping using vsc-based series connected facts controllers," *Generation, Transmission and Distribution, IEE Proceedings-*, vol. 150, no. 3, pp. 353 – 359, may 2003.

[6] L. Rouco, "Design of damping controllers of static series voltages source using eigenvalue sensitivities," in *Transmission and Distribution Conference and Exposition, 2001 IEEE/PES*, vol. 1, 2001, pp. 8 –13 vol.1.

[7] S. Bamasak and M. Abido, "Assessment study of shunt facts-based controllers effectiveness on power system stability enhancement," in *Universities Power Engineering Conference, 2004. UPEC 2004. 39th International*, vol. 1, sept. 2004, pp. 274 –278 Vol. 1.

[8] Y. Tan, "Analysis of line compensation by shunt-connected facts controllers: a comparison between svc and statcom," *Power Engineering Review, IEEE*, vol. 19, no. 8, pp. 57 –58, aug 1999.

[9] S. Jiang, A. Gole, U. Annakkage, and D. Jacobson, "Damping performance analysis of ipfc and upfc controllers using validated small signal models," in *Power and Energy Society General Meeting, 2011 IEEE*, july 2011, p. 1.

[10] J. Veeramalla and R. Sreerama Kumar, "Application of interline power flow controller (ipfc) for damping low frequency oscillations in power systems," in *Modern Electric Power Systems (MEPS), 2010 Proceedings of the International Symposium*, sept. 2010, pp. 1 –6.

[11] B. Johnson, "How series and combined multiterminal controllers facts controllers function in an ac transmission system," in *Power Engineering Society General Meeting, 2004. IEEE*, june 2004, pp. 1265 –1267 Vol.2.

[12] G. Kumar and M. Kalavathi, "Cpf, tds based voltage stability analysis using series, shunt and series-shunt facts controllers for line outage contingency," in *Power and Energy Systems (ICPS), 2011 International Conference on*, dec. 2011, pp. 1 –6.

[13] C. Schauder, M. Gernhardt, E. Stacey, T. Lemak, L. Gyugyi, T. Cease, and A. Edris, "Development of a plusmn;100 mvar static condenser for voltage control of transmission systems," *Power Delivery, IEEE Transactions on*, vol. 10, pp. 1486 –1496, 1995.

[14] L. Gyugyi, C. Schauder, and K. Sen, "Static synchronous series compensator: a solid-state approach to the series compensation of transmission lines," *Power Delivery, IEEE Transactions on*, vol. 12, pp. 406 –417, 1997.

[15] K. Sen, "Sssc-static synchronous series compensator: theory, modeling, and application," *Power Delivery, IEEE Transactions on*, vol. 13, pp. 241 –246, 1998.

[16] A. Nabavi-Niaki and M. Iravani, "Steady-state and dynamic models of unified power flow controller (upfc) for power system studies," *Power Systems, IEEE Transactions on*, vol. 11, pp. 1937 –1943, 1996.

[17] Y. Tan, "Analysis of series and shunt line compensation by a unified power flow controller," *Power Engineering Review, IEEE*, vol. 19, no. 9, pp. 63 – 64, sept. 1999.

[18] L. Gyugyi, C. Schauder, S. Williams, T. Rietman, D. Torgerson, and A. Edris, "The unified power flow controller: a new approach to power transmission control," *Power Delivery, IEEE Transactions on*, vol. 10, pp. 1085 –1097, 1995.

[19] L. Gyugyi, K. Sen, and C. Schauder, "The interline power flow controller concept: a new approach to power flow management in transmission systems," *Power Delivery, IEEE Transactions on*, vol. 14, pp. 1115 –1123, 1999.

[20] P. Kundur, J. Paserba, and S. Vitet, "Overview on definition and classification of power system stability," in *Quality and Security of Electric Power Delivery Systems, 2003. CIGRE/PES 2003. CIGRE/IEEE PES International Symposium*, 2003, pp. 1 – 4.

[21] C. Sharma and M. G. Ganness, "Determination of power system voltage stability using modal analysis," in *Power Engineering, Energy and Electrical Drives, 2007. POWERENG 2007. International Conference on*, 2007, pp. 381 –387.

[22] C. Karawita and U. Annakkage, "Multi-in-feed hvdc interaction studies using small signal stability assessment," in *Power Energy Society General Meeting, 2009. PES '09. IEEE*, july 2009, p. 1.

[23] D. H. R. Suriyaarachchi, U. D. Annakkage, C. Karawita, and D. A. Jacobson, "A procedure to study sub-synchronous interactions in wind integrated power systems," *Power Systems, IEEE Transactions on*, vol. PP, no. 99, p. 1, 2012.

[24] S. Limyingcharoen, "Applications of unified power flow controllers in power system stability enhancement," Ph.D. dissertation, Department of Electrical and Electronic Engineering, University of Auckland, 1999.